Recovery of metals in a double-stage continuous bioreactor for acidic bioleaching of printed circuit boards (PCBs)

Agathe Hubau, Michel Minier, Alexandre Chagnes, Catherine Joulian, Charline Silvente, Anne-Gwenaëlle Guezennec

Recovery of metals in a double-stage continuous bioreactor for acidic bioleaching of printed circuit boards (PCBs)

Agathe HUBAU[1,2 *], Michel MINIER[2], Alexandre CHAGNES[3], Catherine JOULIAN[1], Charline SILVENTE[1], Anne-Gwenaëlle GUEZENNEC[1]

[1]BRGM, F-45060 Orléans, France

[2]Chimie ParisTech, PSL Research University, CNRS, Institut de Recherche de Chimie Paris (IRCP), F-75005 Paris, France

[3] Université de Lorraine, CNRS, GeoRessources, F- 54000 Nancy, France

* Corresponding author E-mail address: a.hubau@brgm.fr

Abstract

Many studies are now focusing on bioleaching methods to recover metals from WEEE. The efficiency of this process is highly dependent on microorganisms but also on the solid-liquid-gas mass transfer, which is controlled by the reactor design. In this study, bioleaching of comminuted spent printed circuit boards (PCBs) was performed in a stirred tank reactor operated in batch mode and in a double-stage continuous bioreactor. The metal dissolution kinetics were compared. The first stage of the continuous bioreactor was a bubble column in which a BRGM-KCC acidophilic consortium comprising *Leptospirillum ferriphilum* and *Sulfobacillus benefaciens* was used to oxidise Fe(II) into Fe(III). The resulting liquor was used to leach out metals contained in PCBs in the second stage of the bioreactor with mechanical stirring. The use of two distinct stages allowed the bacteria to adapt gradually to the PCBs and reach high dissolution yields, *i.e.* 96% Cu, 73% Ni, 85% Zn and 93% Co when 1% (w/v) PCB scraps were added into the bioleaching reactor, with a hydraulic residence time of 48 hours. By using the double-stage bioreactor, the concentration of PCB scraps could be increased up to 1.8% (w/v) without reducing bioleaching performance. Biomass concentration in the second stage and adaptation of the microorganisms to the toxicity of the metals were sufficient for only the second stage to be used. Under these conditions, the dissolution kinetics were stable, even when iron was provided only by the comminuted PCBs.

Keywords: Bioleaching / WEEE / acidophilic microorganisms / Printed Circuit Boards

1. Introduction

Hydrometallurgy to recover valuable metals involves three main stages: leaching, purification and recovery. This technique has many advantages compared to pyrometallurgy, including lower energy consumption, capital costs and gas emissions. (Tuncuk et al., 2012). However, conventional hydrometallurgical processes consume large quantities of chemicals. The use of microorganisms to recover metals, known as bio-hydrometallurgy, is an economic and environmentally sound alternative. Bioleaching, which is one of the most frequently studied unit operations in biohydrometallurgy, allows the amounts of reagents to be substantially reduced because they are produced *in situ* by microorganisms under soft operating conditions, *i.e.* low temperatures and a mild pH (Mrážiková et al., 2016). Bioleaching is an established commercial technology that has been applied worldwide for over half a century to process concentrates and mineral processing wastes. More recently, it has been recognised as a promising technology for the treatment of e-wastes, and more particularly of spent Printed Circuit Boards (PCBs). These wastes contain approximately 40% of metals, 30% of plastics and 30% of glass and oxides (Sum, 1991). Metal concentrations in PCBs, including precious and base metals, are generally higher than those found in primary resources. Therefore, there is considerable interest in developing efficient, soft and sustainable methods to recover these metals (Tuncuk et al., 2012).

The first study on PCB bioleaching was published by Brandl et al. (2001) and relied on the use of acidophilic microorganisms. The two main reactions that occur are:

$$M^0 + zFe^{3+} \rightarrow M^{z+} + zFe^{2+} \quad [1]$$

$$2Fe^{2+} + 0.5O_2 + 2H^+ \rightarrow 2Fe^{3+} + H_2O \text{ (bacteria)} \quad [2]$$

Metals are oxidised by Fe(III), which is reduced into Fe(II) (Eq. (1)). Fe(III) is then regenerated by the bacteria in the presence of dissolved oxygen according to Eq. (2). Fe(II) oxidation in the absence of bacteria is slow but the presence of ferro-oxidising bacteria in the bioleaching processes significantly accelerates Fe(III) regeneration. Brandl et al. (2001) showed that one or more elements contained in PCBs may be sufficiently toxic to acidophilic cultures to cause a dramatic decrease in bioleaching efficiency. Therefore, several works in the literature have focused their studies on the feasibility of PCB bioleaching in batch mode by using shake flasks and bioreactors (Bas et al., 2013; Guezennec et al., 2015; Ilyas et al., 2010). A comparison of these studies brings out several points. Firstly, the time needed for microorganisms to adapt to toxic elements in PCBs can vary depending on the PCB composition and is dependent on the specificity of the microbial strains present. Secondly, it

is very difficult to draw clear conclusions from the studies reported in the literature because the experiments were performed under very different operating conditions. For example, the initial PCB content in the reactor varies from less than 1% (w/v) to more than 10% (w/v) and the particle size distribution can be quite different from one study to another. Furthermore, the very large discrepancies in bioleaching efficiency and bioleaching rates observed by comparing the different studies may arise from:

- Sampling issues: most of the experiments were performed with very small amounts of PCBs, which can entail sample representativeness and reproducibility problems (Gy, 1992; Bryan et al., 2015).
- Mass transfer issues due to the complex nature of bioleaching systems that involve gas-liquid-solid interfaces. For instance, difficulties in controlling dioxygen concentrations in the liquid phase may be responsible for discrepancies between bioleaching rates, especially when the experiments are carried out in flasks rather than in appropriate bioreactors (Hubau et al., 2018).

Consequently, PCB bioleaching should preferably be investigated in large stirred tank reactors (>1L), in which significant amounts of samples can be processed and the transport of reactants is more efficient.

Most of the studies also show that staggering the biological production of a lixiviant acidic solution containing Fe(III) and the addition of PCBs increases bioleaching efficiency, probably by lowering the toxicity of PCBs for microbial growth (Liang et al., 2013, Brandl et al., 2001).

Figure 1 shows Cu dissolution kinetics determined in studies addressing PCB bioleaching (Adhapure et al., 2013; Arshadi and Mousavi, 2014; Arshadi and Mousavi, 2015; Bai et al., 2009; Bai et al., 2016; Bas et al., 2013; Brandl et al., 1999; Bryan et al., 2015; Chen et al., 2015; Choi et al., 2004; Gu et al., 2014; Gu et al., 2017a; Gu et al., 2017b; Guezennec et al., 2015; Ilyas et al., 2007; Ilyas et al., 2010; Ilyas et al., 2013; Ilyas et Lee, 2014; Işildar et al., 2015; Liang et al., 2010; Liang et al., 2013; Liang et al., 2016; Mäkinen et al., 2015; Mrážiková et al., 2013; Mrážiková et al., 2015; Mrážiková et al., 2016; Nie et al., 2014; Nie et al., 2015; Priya and Hait, 2018; Rodrigues et al., 2015; Shah et al., 2014; Shah et al., 2015; Silva et al., 2015; Sodha et al., 2017; Wang et al., 2009; Wang et al., 2016; Wang et al., 2018; Willner 2013; Willscher et al., 2007; Xia et al., 2017; Xiang et al., 2010; Yamane et al., 2018; Yang et al., 2009; Yang et al., 2014; Zhu et al., 2011). The figure shows that the highest Cu

dissolution kinetics are obtained when microorganisms and PCBs are added separately rather than simultaneously. Several authors have suggested that the use of a two-stage process is a promising option (Brandl et al., 2001). Such a process has already been used for processing spent Ni-Cd batteries (Cerruti et al., 1998) but never to leach metals from PCBs, to our knowledge.

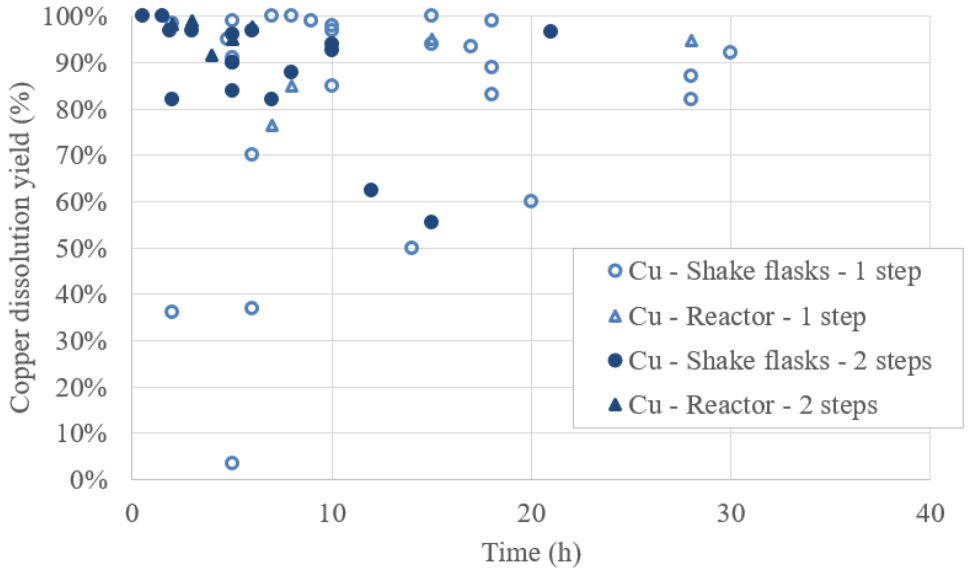

Figure 1: Copper dissolution yields over time reported by several studies in batch mode and depending on whether the study was carried out in a flask or in a reactor, and in one stage (inoculum and PCBs added simultaneously) or two (inoculum and PCBs added separately).

For this study, a double-stage bioreactor was designed in order to bioleach comminuted PCBs in continuous mode. This configuration was chosen to reduce the impact of PCB toxicity on microbial growth and activity and to improve bioleaching efficiency. The first stage dedicated to iron bio-oxidation is described in our previous study (Hubau et al., 2018). The present paper focuses on the second stage of the bioreactor where bioleaching of comminuted spent PCBs is performed in order to optimise its operation in continuous mode and improve the metal dissolution kinetics. Particular attention is given to the resistance of microorganisms to PCBs by performing experiments in batch mode using shake flasks.

2. Material and methods

2.1 Growth medium and bacterial culture.

The BRGM-KCC bacterial acidophilic consortium was used for this study. The predominant microorganisms were affiliated to the genera *Leptospirillum*, *Acidithiobacillus* and

Sulfobacillus, which oxidise either iron or sulphur, or both (Guezennec et al., 2017). The inoculum used in the experiments originated from the BRGM cultures collection and was subcultured several times on pyrite. The nutrient medium was denoted 0Cm and made up of 0.4 $g.L^{-1}$ $(NH_4)_2SO_4$ (extrapure, Merck), 0.81 $g.L^{-1}$ H_3PO_4 85% (analytical grade, Merck), 0.48 $g.L^{-1}$ KOH (pure pellets, Merck) and 0.52 $g.L^{-1}$ $MgSO_4.7H_2O$ (analytical grade, Merck). This medium was chosen since it enabled to obtain high performances of biooxidation in the bubble column, with stable biooxidation rate and yield, and microbial growth (Hubau et al., 2018). Ferrous sulphate was added when needed as $FeSO_4.7H_2O$ (99+%, Acros Organics). Concentrated sulphuric acid (> 95%, analytical grade, Fisher Chemical) was used to adjust the pH to 1.3.

2.2 Printed Circuit Board samples.

A sample of 526 kg of medium-grade spent PCBs in the Small Waste Electrical and Electronic Equipment category (sWEEE) was collected from small appliances, such as IT equipment, audio and video appliances, toys, personal care products, kitchen appliances, *etc*., all provided by the "Envie 2E Midi-Pyrénées" WEEE sorting centre (France). The PCBs were shredded to 750 µm using a shear shredder (Bohmier Maschinen GmbH) and a laboratory knife mill (Retsch SM-2000). The detailed procedure is described in Hubau et al., 2019. The samples were divided successively to obtain smaller samples using a quartering methodology. Figure 2 shows the particle size distribution of the final samples, determined by wet sieving of 290 g of comminuted PCBs.

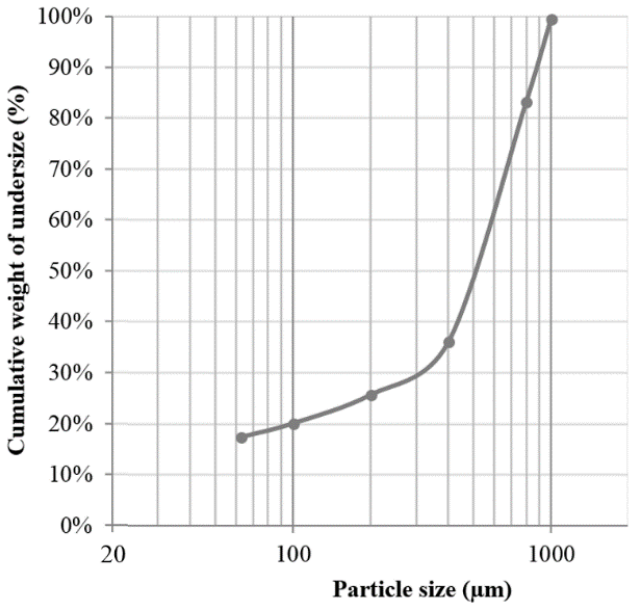

Figure 2: Particle size distribution of comminuted PCBs shredded with a shear shredder (Bohmier Maschinen GmbH) and a laboratory knife mill (Retsch SM-2000) equipped with a bottom sieve mesh size of 750 µm.

To determine metal concentrations, a triplicate of 40 g samples of shredded PCBs was leached at 200 °C for 2 hours in a Kjeldatherm-Gerhardt digestion system with 450 mL of aqua regia HNO_3:HCl 1:3 prepared by mixing 112 mL of 67-69%(mol.) HNO_3 (trace metal grade, Fisher Chemical) and 336 mL of 32%(mol.) HCl (certified for analysis, Fisher Chemical). After filtration, the leachates were analysed with a Varian SpectrAA-300 flame atomic absorption spectroscope (FAAS) to determine Fe, Cu, Zn, Pb, Ni and Co concentrations. The leachates were also analysed with an ICP-OES Horiba Jobin Yvon Ultima 2 or an ICP-MS Thermo Scientific X Series to determine concentrations of minor elements (Ag, Al, Au, Cr, Ga, Ge, In, Mg, Mo, Mn, Pd, Pt, Sb, Sn, Ta, V and W). The metal concentrations are given in Table 1: the concentrations for Cu, Fe, Zn, Pb, Ni and Co were the average values of a triplicate; for Al, Sn, Ag, Au, Pd, Ga and Ta, they were the average values of a duplicate; the concentrations of other elements were measured from a single sample.

Element	Concentration (% weight)
Cu	14.58%
Fe	12.23%
Al	6.04%
Zn	1.67%
Sn	1.67%
Pb	1.17%
Mn	0.61%
Ni	0.34%
Sb	0.20%
Mg	0.14%

Element	Concentration ($mg.kg^{-1}$)
Cr	842
Co	358
Ag	209
Mo	152
In	100
Au	44
Pd	25
V	22
W	15
Ga	12
Ta	7.5
Ge	0.75
Pt	0.59

Table 1: Concentrations (in % weight and mg.kg^{-1}) in PCB samples (weight = 40 g). The samples were leached by aqua regia at 200 °C at a liquid/solid ratio of 11 mL.g^{-1} (N.A.=not analysed).

2.3 Evaluation of toxicity in shake flasks.

To evaluate the impact of cations from PCBs on the growth and activity of the bacteria, the kinetics of Fe(II) bio-oxidation in the presence of different proportions of PCB leachate in the culture medium were measured. The experiments were carried out in 250 mL Erlenmeyer flasks. The leachate was prepared by abiotic leaching of PCBs (5%(w/v)) in the presence of 9 g.L^{-1} of synthetic Fe(III) added as $Fe_2(SO_4)_3.xH_2O$ (reagent grade from Alfa Aesar). Leaching was performed in a 2-L stirred tank reactor (STR) at 36 °C for 20 days. Analytical techniques (described in Section 2.6) were used to determine the pH value, redox potential and metal concentrations. After filtration through Whatman filters with 2.7 µm cotton fibres, the final metal concentrations in the leachate were analysed (Table 2). Other metals such as Al were assumed to be present in the leachate but their concentrations were not determined. This leachate was then mixed in different proportions with water acidified to pH 1.3 with sulphuric acid (0% v/v, 10% v/v, 30% v/v and 60% v/v). Nutrients were added into each flask (same quantities for all tests, equivalent to 0Cm nutritive medium concentrations), as well as ferrous sulphate so that the initial Fe(II) concentrations were above 6 g.L^{-1}. The flasks were then inoculated with 10 mL (10% v/v) of BRGM-KCC consortium containing 1 g.L^{-1} Fe(II) and 10^7 cell.mL^{-1}. The flasks were maintained in an incubator at 40 °C and 107 rpm, with pH values and redox potential measured on a daily basis.

Metal	Leachate concentration (mg.L^{-1})
Cu	9 416
Fe	16 840
Zn	934
Pb	16.8
Ni	18.7
Co	17.9

Table 2: Concentrations (in mg.L^{-1}) of Cu, Fe, Zn, Pb, Ni and Co in the leachate used for evaluating toxicity in shake flasks.

2.4 PCB bioleaching in batch mode.

➢ *Experimental setup*

The PCB bioleaching experiments in batch mode were performed in laboratory-scale glass bioreactors with a working capacity of 2.25 L and jacketed for warm water circulation to maintain a constant operating temperature (Figure 3). The temperature of the circulating water was regulated by a cryothermostat and thermocouples placed in the bioreactors. The bioreactors were equipped with four baffles mounted 90° apart and extending down to the base of the vessel to optimise mixing of the pulp. The agitator was a dual impeller system (axial/radial) consisting of a standard 6-blade Rushton turbine in combination with a 3-blade 45° axial flow impeller. The gas supply system was designed to accommodate air enriched with 1% CO_2, which was injected beneath the turbine at the bottom of the bioreactors via a stainless steel pipe. The impellers and the gas injection pipe were positioned so as to keep to the standard dimensions and thus optimise gas mass transfer and mixing in the bioreactors. The top of the reactors was connected to a gas cooling system to prevent excessive evaporation.

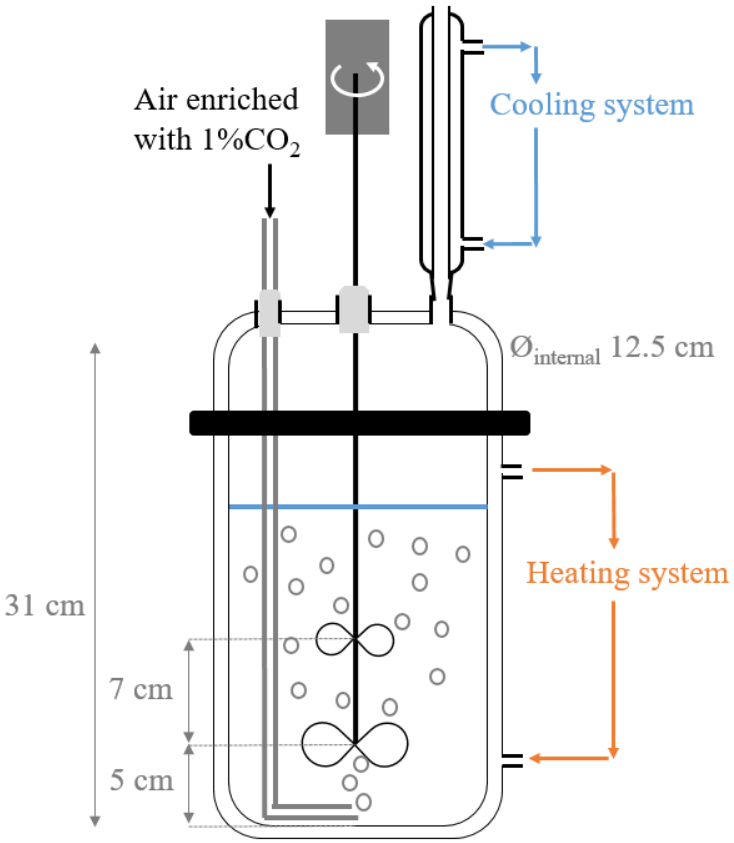

Figure 3: Schematic diagram of the experimental setup for bioleaching tests in batch mode.

- *Methodology and operating conditions during the different experiments*

Two types of tests were performed: abiotic and biotic. During the abiotic tests, acidified water (pH 1.3 with sulphuric acid) and Fe(III) as ferric sulphate was introduced into the bioreactor before adding different quantities of PCBs. When the biotic tests were performed, the consortium (10% v/v) was inoculated in a nutrient medium with synthetic ferrous sulphate. When the redox potential reached 800 mV vs SHE (corresponding to 90% of bio-oxidized Fe(II)), different quantities of PCBs were added. The pH value was adjusted manually to 1.5 with sulphuric acid when it rose above 1.8. Ultrapure water was also added during daily monitoring to compensate for water losses due to evaporation, despite the presence of a condenser.

Different tests were performed to determine the influence of the presence of bacteria and the impact of the initial concentration of Fe(III). The operating conditions that were used are given in Table 3.

Solid concentration	**[Fe(III)] ($g.L^{-1}$)**	**Inoculation**	**Gas flow ($L.h^{-1}$)**	**CO_2 enrichment**	**Temperature (°C)**	**Stirring speed (rpm)**
1% w/v PCBs	8	No	18	0%	40	600
		Yes	60	1%	35	600
	1	No	60	1%	35	600
		Yes	60	1%	35	600
		Yes	60	1%	35	600
	0	No	60	1%	35	600
5% w/v PCBs	8	No	18	0%	40	600
		Yes	60	1%	35	600

Table 3: Operating conditions during abiotic and biotic leaching experiments of comminuted spent PCBs in 2.25 L-STR operated in batch mode.

Metal dissolution rates reported in this study were calculated as the maximum slope of metal concentration vs. time obtained during batch experiments. For some experiments, two values were reported since two distinct slopes, corresponding to two successive phenomena, were observable.

2.5 PCBs bioleaching in continuous mode

Bioleaching experiments in continuous mode were carried out in the double-stage bioreactor, illustrated in Figure 4.

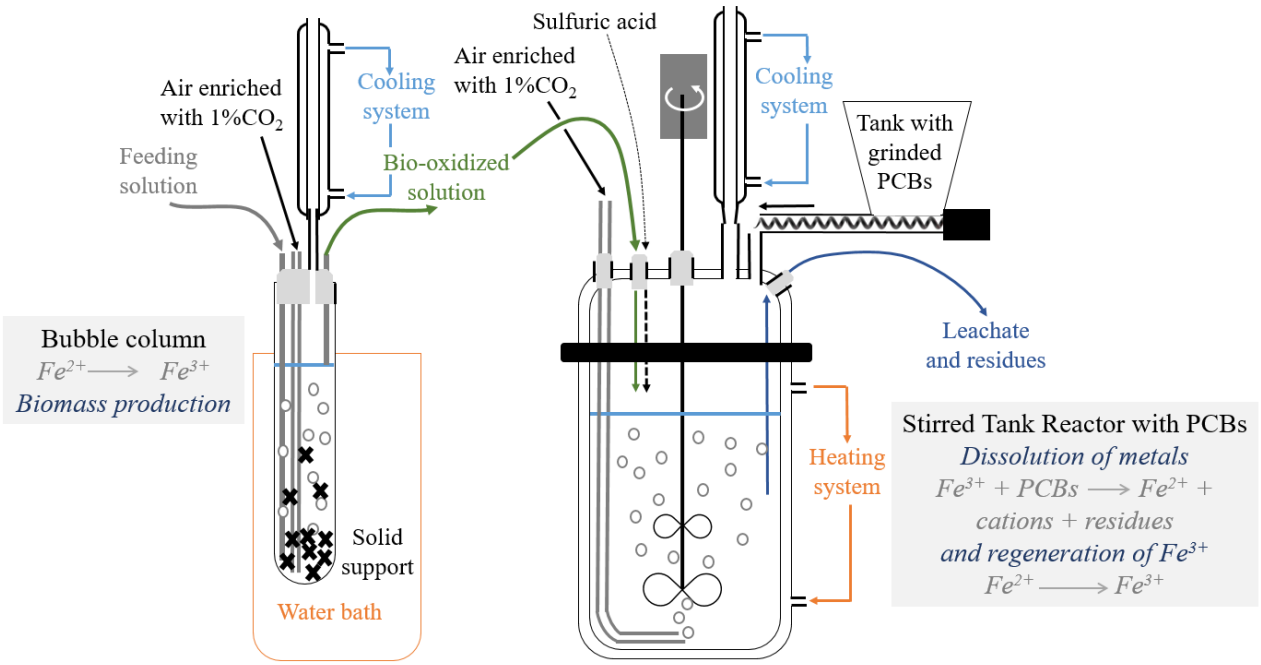

Figure 4: Schematic diagram of the continuous double-stage bioreactor used for PCB bioleaching.

The first stage was described in detail in our previous paper (Hubau et al., 2018). The 200 mL-bubble column was filled with 150 mL of 0Cm medium containing 1 $g.L^{-1}$ Fe(II) from ferrous sulphate at pH 1.1 and 15 g of activated charcoal (Organosorb11® from Desotec, high specific surface area=950 $m^2.g^{-1}$). Prior to use, the activated charcoal was washed with 5 $mL.g^{-1}$ of water and 1 $mL.g^{-1}$ of diluted sulphuric acid (pH 1.3), then dried at 40 °C for 20 hours and sieved to remove particles smaller than 1 mm. Bubble column stirring was performed by means of a continuous air flow enriched with 1% of CO_2 (air flow rate= 20-30 $L.h^{-1}$ at 1 bar relative to atmospheric pressure and ambient temperature). The CO_2 enrichment was performed since it was previously proven that it favoured the growth and activity of BRGM-KCC consortium (Guezennec et al., 2018). The temperature of the bubble column was maintained at 36 °C by means of a thermostatic bath (Lauda), since this temperature was close to the optimal temperature for the growth and activity of *Leptospirillum ferriphilum*, one of the predominant strain of BRGM-KCC consortium that is able to oxidize iron (Coram and Rawlings, 2002). The hydraulic residence time (HRT) was set to 3.2 hours. Continuous feeding of the bioreactor and continuous removal of the effluent were performed at the desired dilution rate by variable-speed pumps. The bubble column was first inoculated with

the BRGM-KCC consortium at 10% (v/v) in batch mode. Once the redox potential reached 900 mV vs SHE, the bubble column was run in continuous mode. HRT was gradually decreased to 3.2 hours. All experiments were performed without sterilisation to be as representative of industrial conditions as possible.

The second stage was a 2.25 L-STR fed continuously with the leaching solution produced in the bubble column. This STR was the same as the one used in batch mode, described in Section 2.4. The incoming flowrate was set at 47 $mL.h^{-1}$ so that HRT in the STR was 48 hours. The STR was also fed with comminuted spent PCBs by means of a dosing screw (from Dosapro Milton Roy) controlled with a programmable logic controller (Siemens LOGO!). The flowrate of solids could vary between 0.5 and 0.85 $g.h^{-1}$ so that the PCB concentration varied from 1%(w/v) to 1.8%(w/v). The outflow (pulp) was removed with a peristaltic pump. To adjust the pH to 1.5, sulphuric acid was added with a peristaltic pump at concentrations ranging from 1.8 to 3.5 $mol.L^{-1}$ and a flow rate of 2 to 5 $mL.h^{-1}$. STR stirring speed was set at 600 rpm, the temperature was maintained at 36 °C and air flowrate was set to 60 $L.h^{-1}$ with 1% CO_2 enrichment.

At the end of the experiments, the bubble column was by-passed to evaluate the dissolution kinetics of metals from PCBs in a one-stage continuous bioreactor (2.25 L-STR). In this case, the feeding solution did not contain Fe, so that PCBs were the only source of Fe. The feeding solution was composed of 0Cm medium with diluted sulphuric acid to maintain the pH at 1.1.

2.6 Analytical techniques.

pH values and redox potentials were measured daily for all experiments. Metal concentrations (Cu, Fe, Zn, Ni, Co, Pb) in liquid phase were determined by atomic absorption spectroscopy (AAS) using a Varian SpectrAA-300. The Yue et al. (2016) correlation was used to determine the Fe(III) to Fe(II) concentration ratio from the redox potential measurement and the Fe(II) concentration from total Fe concentration. This correlation is not affected by the presence of dissolved metals from PCBs.

When stable characteristics of STR outflow were obtained in continuous mode, concentrations of Ag, Al, Ca, Cr, Ga, K, Mg, Mo, Na, P, S, Sb, Sn, Ta, V and W in the STR liquid phase were measured with ICP-OES (following the ME-ICP02 protocol of the ALS company in Loughrea, Ireland). NH_4^+ concentration was also measured in these samples by colorimetric assays in accordance with the NF ISO 15923-1 standard (AFNOR, 2014). Concentrations of solids were also determined to validate the experimental setup. XRD was

used on the bioleaching residues (Bruker D8 Advance diffractometer, 4-75 °2θ, 0.03 °2θ/s, 288 s each step, Cu tube) and the diffraction patterns were processed with Diffrac Suite software.

2.7 Bacterial community monitoring.

2.4.1 Cell counting. The bacterial cells were counted in the liquid phase of the different experiments with a Thoma cell counting chamber.

2.4.2 Scanning electron microscopy (SEM) with lyophilisation. SEM was used to observe microorganisms being attached to PCB particles during the experiments in continuous mode. For these observations, fresh aliquots of the outflow from the STR bioreactor were sampled. Large particles of PCBs from these pulp samples were introduced onto a copper frame with carbon paste and immersed in liquid nitrogen at -176 °C. Slush nitrogen at -210 °C was reached by pressure depression. The samples were then set into a vacuum, transferred into the SEM (Hitachi S-4500 field-emission) and slowly warmed up to room temperature. They were then coated with Au-Pd alloy to obtain electrically conductive samples whatever the composition of the PCB particle, and finally observed under a secondary electron beam at 2 kV. Energy dispersive X-ray spectroscopy (EDX) was used to characterise the sample composition with SEM operated at 15 kV.

2.4.3 DNA extraction, 16S rRNA gene PCR (polymerase chain reaction) amplification and bacterial community fingerprints. Samples of 0.5 mL solid medium or 2 mL liquid phase were taken from the bubble column; 5 mL pulp samples were taken from the stirred tank reactor. The solid samples, pulp and pellets (from centrifuging the liquid samples for 10 minutes at 14000 g) were washed by re-suspension in Tris buffer (100 mM, pH 8) until a pH around 7 was reached. Genomic DNA was extracted with the FastDNA Spin Kit for Soil, using the manufacturer's protocol (MP Biomedicals) with a FastPrep®-24 at a speed of 5 $m.s^{-1}$ for 30 s (lysis was performed twice for the activated charcoal samples). PCR amplification of the 16S rRNA genes (ca. 200 bp) from DNA extracts was performed with the w49 forward primer and the 5'-end FAM-labelled w34 primer, in a C-1000 thermocycler (Biorad), as described in Hedrich et al. (2016). The amplification products were analysed on agarose gel. Community fingerprints were obtained by CE-SSCP (Capillary electrophoresis-single strand conformational polymorphism). One microlitre of 5- to 500-fold diluted PCR product, 0.4 µL of Genescan-600 LIZ internal standard (Applied Biosystems) and 18.6 µL of deionized formamide HiDi (Applied Biosystems) were heat-denatured for 5 minutes at 95 °C and immediately cooled on ice for 10 minutes. Fragment analyses were conducted with the ABI

Prism 310 (Applied Biosystems). GeneScan software (Applied Biosystems) was used to realign the peak profiles based on internal standard migration, assign peak position, align community peaks with peaks of known acidophilic strains, and calculate relative abundances on the basis of peak areas.

3. Results

3.1 Microbial ecotoxicology

The microbial ecotoxicology tests performed in this study to evaluate the toxicity of dissolved cations were carried out with PCB leachate rather than with solid PCBs or synthetic solutions for two main reasons:

(i) When working at a small scale (a few hundred mL), the quantity of PCBs that can be added to a flask is limited to a few grams to correspond to concentrations of less than 10% solids (this is the maximum concentration used in the literature on PCB bioleaching). However, samples of such small size are no longer representative of the initial batch of PCBs and vary widely in their composition, so that the results obtained are difficult to compare. The use of a leachate obtained from a large quantity of PCBs allows work to be done at a small scale in a repeatable and representative manner.

(ii) The toxicity evaluation performed with leachates takes the impacts of both major metals and metal traces into account. This is a great advantage in comparison to synthetic solutions that could be prepared to model PCB cations.

Figure 5 shows that biomass growth and Fe(II) bio-oxidation were delayed when the leachate proportion increased. The duration of the lag phase increased with the quantity of leachate. However, despite this delay, the maximum bio-oxidation rate and the final biomass concentration were of the same order of magnitude as in the absence of leachate (around 200 $mg.L^{-1}.h^{-1}$ of Fe(II) oxidized and 10^8 $cell.mL^{-1}$ respectively). Thus, regardless of the amount of leachate added, the bacterial culture seemed to adapt progressively to increasing metal concentrations. These results are consistent with those obtained by Choi et al. (2004). The results of our study are promising as regards the ability of the BRGM-KCC consortium to bioleach PCBs. They also confirmed the relevance of separating bacterial growth from the bioleaching of PCBs, in order to limit the lag phase related to the toxicity of PCB cations.

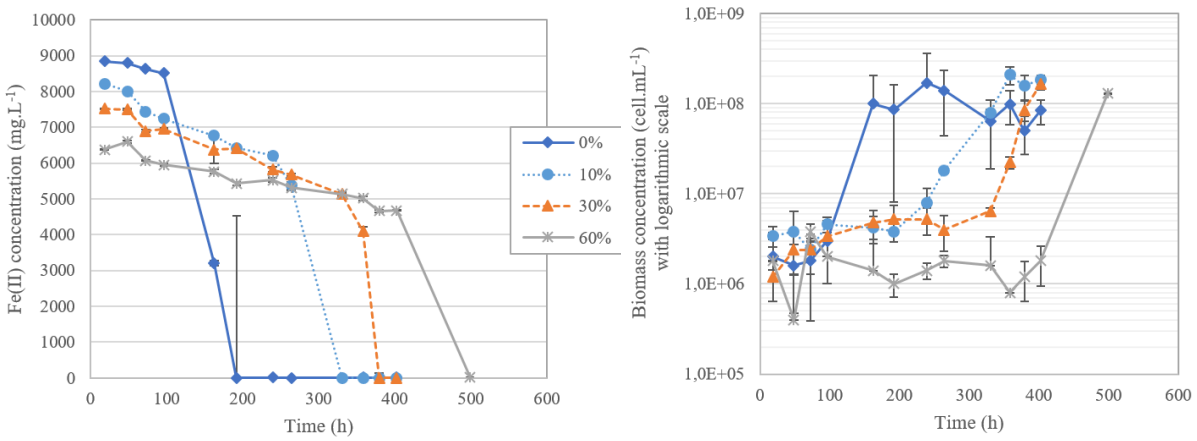

Figure 5: Changes in Fe(II) concentrations (in mg.L^{-1}) and biomass concentrations (in cell.mL^{-1}, logarithmic scale) over time in shake flasks with 0 to 60% of PCB leachate in the culture medium (each experiment was performed in duplicate).

3.2 Abiotic and biotic leaching of PCBs in batch mode

Various experiments were carried out in batch mode to determine the dissolution kinetics of Cu, Fe, Ni, Zn, Pb and Co in the presence of sulphuric acid without microorganisms and Fe(III), in the presence of Fe(III) without microorganisms (abiotic tests) and in the presence of biogenic Fe(III), *i.e.* Fe(III) produced via Fe(II) oxidation by microorganisms. Figure 6 compares Cu and Ni dissolution kinetics at 1%(w/v) under different operating conditions: (i) with sulphuric acid only; (ii) with 1 g.L^{-1} of Fe(III); (iii) with 8 g.L^{-1} Fe(III). Both synthetic and biogenic Fe(III) were used during these tests. Similar pH was maintained during these experiments. Cu dissolution yields were higher than 100% due to a probable underestimation of Cu content in PCBs, as reported in Bryan et al. (2015). When the concentration of Fe(III) was high (8 g.L^{-1}), the dissolution kinetics were fast compared to those obtained with 1 g.L^{-1} Fe(III) or with sulphuric acid only. The same results were obtained for Zn and Co (data not shown). For Pb, low dissolution yields were observed under all conditions, probably due to precipitation (data not shown). For Fe, an increase in concentrations, related to the dissolution of Fe contained in PCBs, was measured initially; the subsequent decrease observed was related to precipitation phenomena (data not shown). Overall, these simultaneous phenomena (dissolution and precipitation) could barely be distinguished, so the Fe dissolution yield and rate were not determined. A residual concentration of Fe(III) (about 1 g.L^{-1}) was measured at the end of the tests carried out with 8 g.L^{-1} Fe(III) (Figure 7), which showed an excess quantity of Fe(III). Also to be noted is that the dissolution kinetics were the same in biotic conditions (with Fe(III) obtained from the bio-oxidation of Fe(II)) and in abiotic conditions

(in the presence of ferric sulphate). However, regeneration of Fe(III) by bio-oxidation of Fe(II) was observed in the biotic experiments after a time-lag that was variable (Figure 7) but longer than the time required for the chemical dissolution of metals. Fe(III) regeneration in the abiotic experiments with 1 $g.L^{-1}$ Fe(III) was also observed due to contamination.

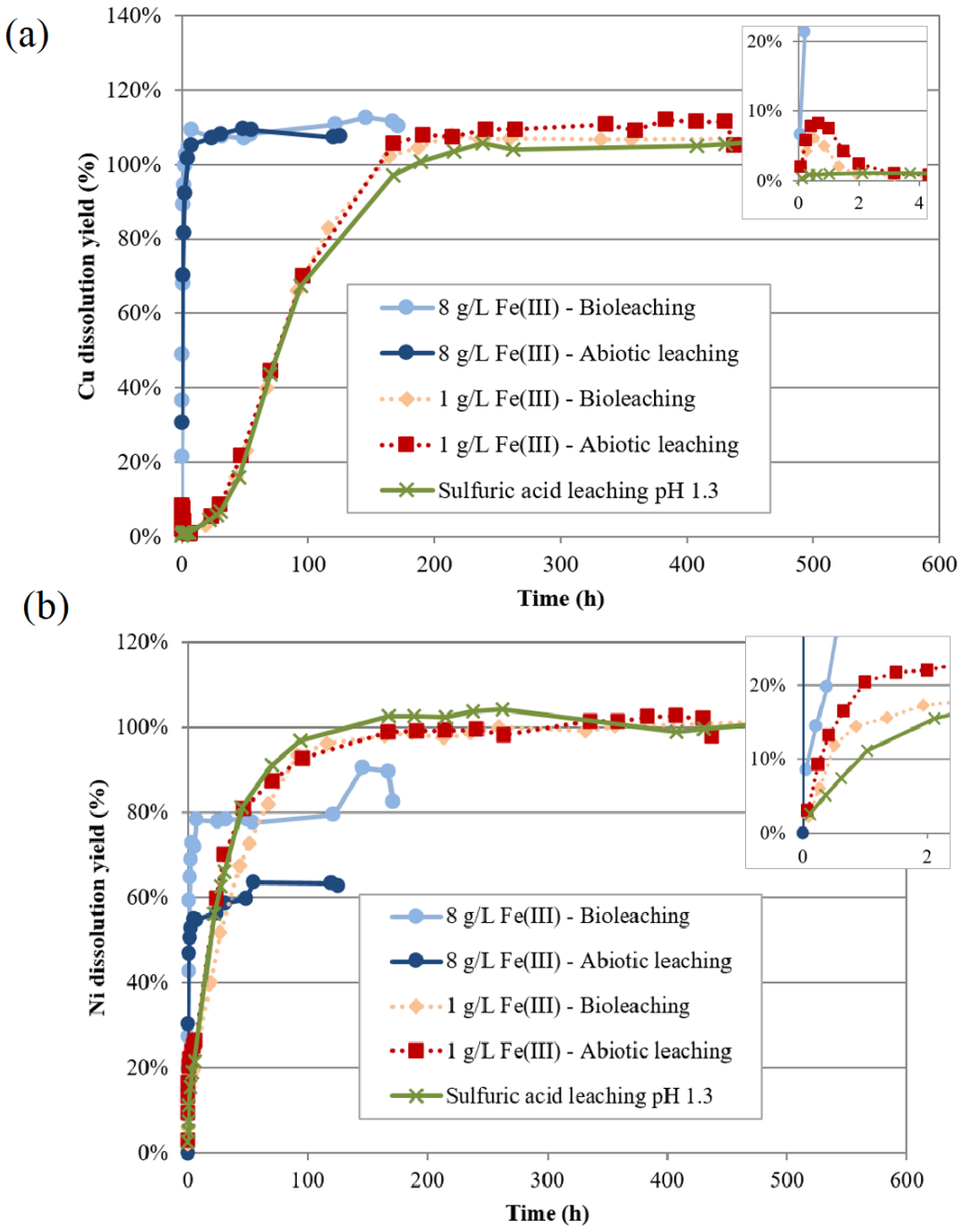

Figure 6: Dissolution yields (in %) over time of (a) Cu and (b) Ni under abiotic and biotic conditions (tests performed in STR operated in batch mode).

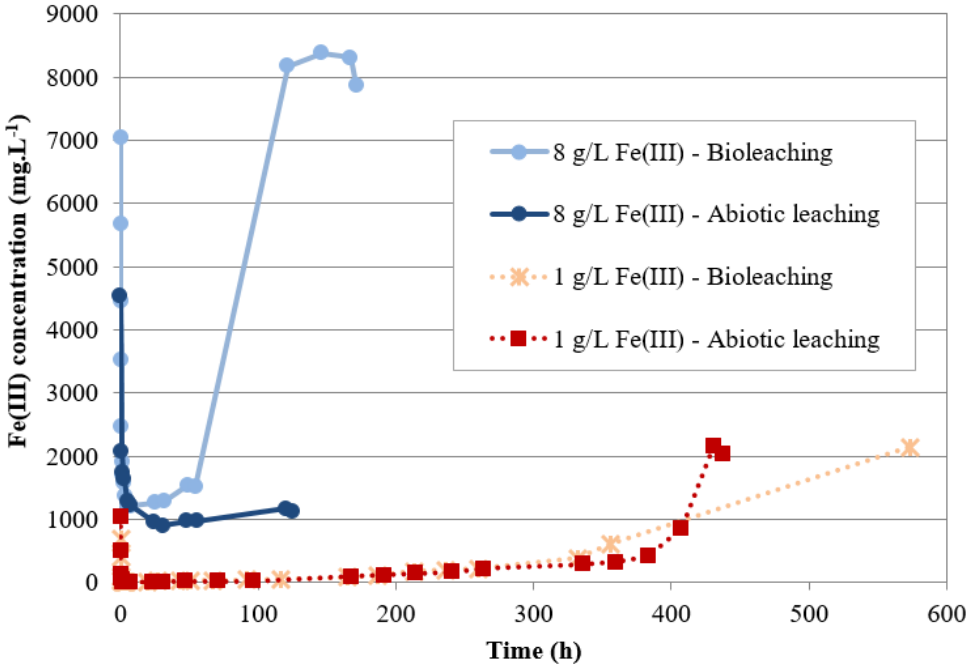

Figure 7: Fe(III) concentrations (in $mg.L^{-1}$) over time in STR operated in batch mode.

The kinetics obtained at 1 $g.L^{-1}$ of Fe(III) were similar to those without Fe. However, in the first hours of the experiments (zooms in the inlet of Figures 6A and 6B), Fe(III) accelerated the dissolution kinetics for major metals but was quickly consumed. The metal dissolution observed after the consumption of Fe(III) was likely to be an acidic hydrolysis. The average proton consumption, measured between the addition of PCBs and the end of metal dissolutions (around 300 h), was 0.4 $mmol.L^{-1}.h^{-1}$. Two different dissolution rates were thus measured (Table 4): in the presence of an excess of Fe(III) and without Fe(III). Except for Pb, the dissolution rates obtained in the presence of Fe(III) were higher than the dissolution rates reached in the second leaching stage (acidic hydrolysis). In the case of Pb, the dissolution rate was probably under-estimated in both leaching stages since Pb precipitated after dissolution. For Cu, an increase followed by a decrease in Cu concentrations was observed at the start of leaching, which could be explained by cementation phenomena.

Metal	Fe(III) dissolution rate ($mg.L^{-1}.h^{-1}$)	H_2SO_4 dissolution rate ($mg.L^{-1}.h^{-1}$)
Fe	1800	500-650
Cu	600	200-250
Zn	115	80
Ni	12	9.3
Pb	10	14

Co	2.7	1.2

Table 4: Dissolution rates (in $mg.L^{-1}.h^{-1}$) observed for Fe, Cu, Zn, Ni, Pb and Co with excess Fe(III) or with sulphuric acid at pH 1.3 in the presence of 1%(w/v) PCBs in batch mode.

Biotic and abiotic tests were also carried out in the presence of 5%(w/v) of solids and 8 $g.L^{-1}$ of Fe(III). Table 5 shows the dissolution rates and yields reached during these experiments. For most metals, very rapid initial dissolution was observed due to the Fe(III) reduction. When all Fe(III) was consumed (low redox potential), dissolution slowed, which probably corresponded to acidic hydrolysis.

Metal	Dissolution yield (%)	Maximum dissolution rate ($mg.L^{-1}.h^{-1}$)
Fe	99%	3200
Cu	104%	2500
Zn	93%	450
Ni	95%	70
Pb	3%	30
Co	92%	13

Table 5: Metal dissolution yields (in %) and rates (in $mg.L^{-1}.h^{-1}$) at 5%(w/v) PCBs with 8 $g.L^{-1}$ of Fe(III) in batch mode.

3.3 Continuous bioleaching of PCBs in a double-stage bioreactor

Continuous bioleaching experiments were carried out with an initial concentration of 1 $g.L^{-1}$ Fe(II) in the feed stream. This operating condition was selected (i) to ensure that Fe(III) was not in excess and that the complete dissolution of PCB metals was made possible by bacterial regeneration of Fe(III), and (ii) to minimise consumption of reagents and simplify the downstream hydrometallurgical purification stages.

The HRT was set at 48 h in the second stage of the bioreactor (PCB leaching in stirred tank reactor), which corresponds to an HRT of 3.2 h in the first stage (bubble column). In these conditions, Fe(II) bio-oxidation performance was stable (100% bio-oxidation and 312 $mg.L^{-1}.h^{-1}$ of Fe(II) bio-oxidized) and biomass concentration was constant over time (2.10^7 $cell.mL^{-1}$) in the first stage (Hubau et al., 2018); the leaching solution that fed the second stage contained 1 $g.L^{-1}$ of Fe(III). This residence time was also selected to allow bacteria to grow in the second stage, since the microbial generation time was shorter than the HRT: Coram and

Rawlings (2002) and Johnson et al. (2008) reported a generation time of 12 - 15 h and 3.1 h for *Leptospirillum ferriphilum* and *Sulfobacillus benefaciens* respectively.

- *Changes in dissolution yields over time in the presence of 1% PCBs*

Although the bioreactor was run at constant operating conditions for 2500 hours, significant changes in redox potential and metal dissolution yields (Figure 8) and pH (Table 6) were observed after 500 and 1600 hours of operation.

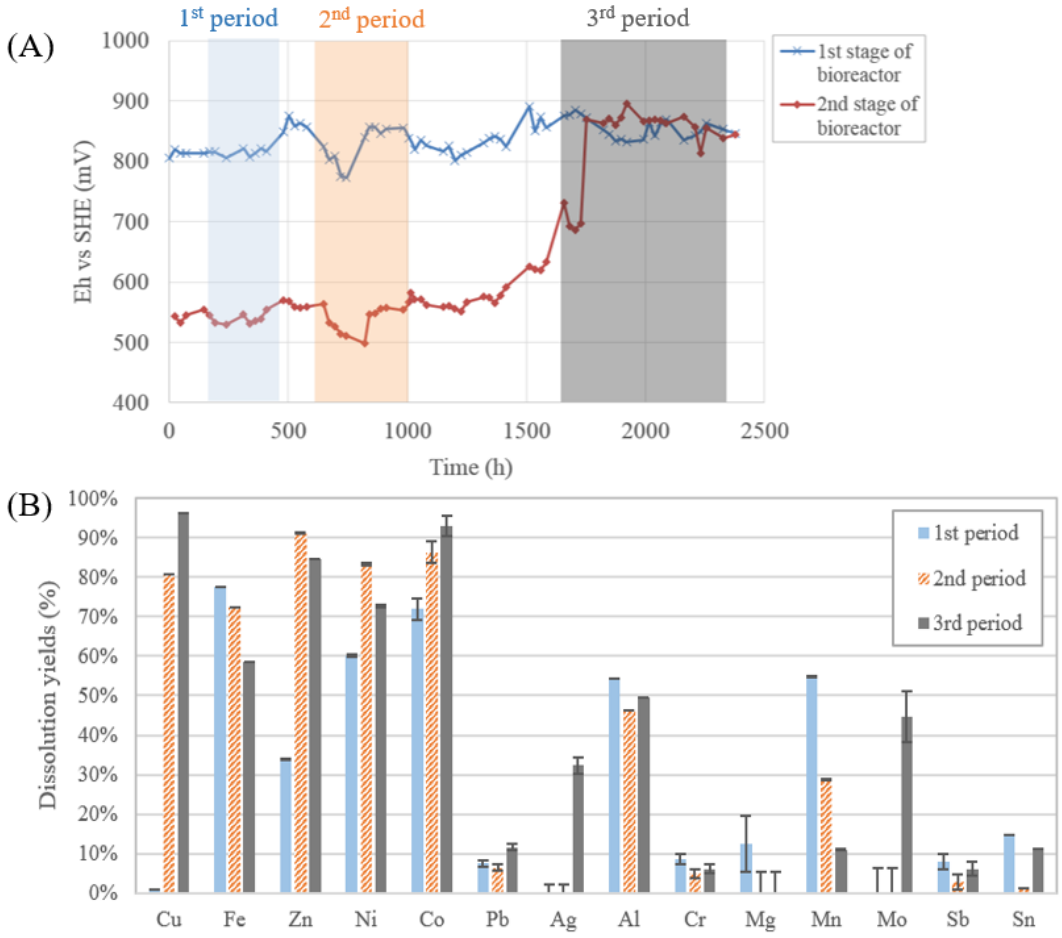

Figure 8: (A) Changes in the redox potential (in mV) in the bioleaching reactor run in continuous mode over time and (B) Metal dissolution yields (in %) in the double-stage bioreactor in the presence of 1%(w/v) of PCBs (continuous mode) depending on the period (error bars depict uncertainties resulting from elemental analyses).

	Period	pH	H^+ consumption in the 2nd stage (mmol.h^{-1})
Feeding solution	-	1.1	-
Outlet of 1st stage	-	1.2	-
Outlet of 2nd stage	Period 1 (0 – 400 h)	1.5	1.7
	Period 2 (600 – 1000 h)	1.8	2.3
	Period 3 (1600 – 2400 h)	> 2.0 so acid added	4.8

Table 6: pH and proton consumption (in mmol.h^{-1}) in the feed solution and at the outlet of the 1st and 2nd stage.

Three leaching periods were defined:

- **Period 1 (0 – 400 h):** The whole amount of incoming Fe(III) from the first stage was reduced as Fe(II) in the 2nd stage (Eh = 530 mV vs SHE). The pH, which was set at 1.1 in the feed solution and was 1.2 at the outlet of the 1st stage, reached 1.5 in the second stage. Cu was not dissolved (<1%), while high yields were obtained for Fe and Co (respectively 76% and 73% dissolution). Limited dissolution yields were obtained for Zn and Ni (respectively 33% and 55%).
- **Period 2 (600 – 1000 h):** Fe was still in the Fe(II) oxidation state but redox potential was slightly higher (Eh = 560 mV vs SHE). In the meantime, acid consumption increased from 1.7 to 2.3 mmol.h^{-1} of protons. The pH reached 1.8 and metal concentrations in the leachate increased significantly. Dissolution yields were respectively 81% Cu, 72% Fe, 91% Zn, 83% Ni and 86% Co.
- **Period 3 (1600 – 2400 h):** Fe(III) was fully regenerated, the redox potential was 880 mV vs SHE. Acid consumption was even greater than during period 2, with a pH value above 2.0. An addition of sulphuric acid was required to limit Fe precipitation (the pH value was maintained at 1.5). Acid consumption reached 4.8 mmol.h^{-1}. Dissolution yields were 96% Cu, 59% Fe, 85% Zn, 73% Ni, 93% Co.

The dissolution rates during these different periods were compared (Table 7). Whatever the period, similar results were obtained for Al dissolution kinetics, with 46% to 54% of Al bioleached. For certain metals in smaller quantities, such as Ag and Mo, a large increase in the bioleaching yield was obtained during the third period; their concentrations were too low to calculate their dissolution rates during the first two periods. In addition, a decrease in the concentration of Mn in the leachate was observed over time and the dissolution yield decreased from 55% in the first period to 10% in the third period, corresponding to a large decrease in the dissolution rate. This result was not yet understood. For Cr, Sb, Sn and Pb, concentrations in the leachate and dissolution rates remained low regardless of the period (dissolution yield <10%). Finally, the limits of detection of Ta, V, W and Ga were higher than the maximum concentration that would be reached if they were completely dissolved, which did not allow us to conclude on the ability to dissolve these metals in these operating conditions.

	Cu	Fe	Zn	Ni	Co	Pb	Ag	Al	Cr	Mn	Mo	Sb	Sn
Period 1	0.26	19.2	1.14	0.41	0.052	0.18	-	6.63	0.015	0.72	-	0.035	0.52
Period 2	23.8	17.9	3.07	0.57	0.063	0.15	-	5.65	0.008	0.37	-	0.013	0.04
Period 3	28.3	12.2	2.71	0.45	0.067	0.28	0.012	6.04	0.010	0.14	0.01	0.027	0.40
+/-	0.02	0.02	0.02	0.02	0.02	0.21	0.008	0.02	0.020	0.02	0.02	0.083	0.21

Table 7: Dissolution rates (in $mg.L^{-1}.h^{-1}$) and errors due to the uncertainties on the analysis of leachate concentrations during PCBs bioleaching in continuous mode in the presence of 1%(w/v) of solids.

- *Consumption of sulphates and precipitation phenomena*

In these complex environments, precipitation phenomena are regularly reported (Adhapure et al., 2013, Ilyas et al., 2010). The X-ray diffractogram of the bioleaching residues (see Supplementary information) revealed the presence of a large quantity of amorphous material, as evidenced by the broad peak located between $2\theta = 12°$ and $2\theta = 30°$. A significant amount of anglesite ($PbSO_4$) was also observed. This explains the low Pb dissolution yields (between 6% and 12%) and is consistent with the literature (Guezennec et al., 2015). Other elements, such as Al and Sn, were also observed in these residues: these were partially dissolved (between 46% and 54% of Al was dissolved and between 1% and 15% of Sn). For Sn, precipitation of SnO during PCB bioleaching has been reported in different studies (Brandl et al., 2001; Bryan et al., 2015). For Al, we can assume that its speciation was very heterogeneous in the sample, with aluminium present as a metal or oxide. Bioleaching was probably not suited to dissolving Al as an oxide, which would account for its detection in the residues.

The X-ray analyses were supplemented by SEM imagery of the residues of bioleached spent PCBs (Figure 9). Crystallization was observed on some particles. EDX analysis suggested that this was potassium jarosite ($KFe_3(OH)_6(SO_4)_2$) that had crystallized on a particle of alumina (Al_2O_3). Traces of Cu were also detected, which could have come from lyophilisation of the leachate containing a high Cu concentration.

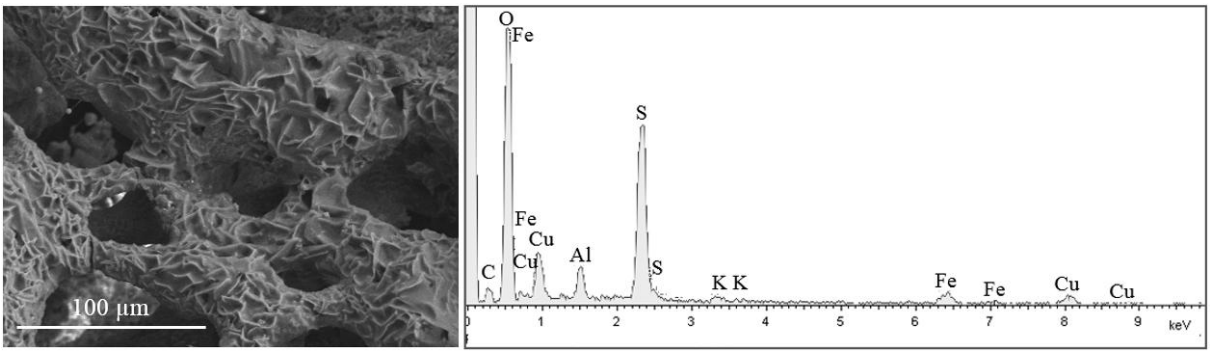

Figure 9: SEM image and EDX analysis of a comminuted spent PCB particle covered with a layer of crystallized precipitate (the particle came from STR reactor during 3rd period).

Jarosite precipitation is common during bioleaching. Fe(III) and sulphates are consumed during this precipitation, according to the following reaction (with A^+ a monovalent cation):

$$A^+ + 3Fe^{3+} + 2SO_4^{2-} + 6H_2O \rightarrow AFe_3(SO_4)_2(OH)_6 + 6H^+ \qquad [3]$$

The precipitation rate was calculated from the concentration of sulphur (only present in solution as sulphates) in the output streams and in the feed stream, with the hypothesis that Fe(III) precipitates mainly in the form of jarosite, with other precipitates, if any, being negligible. This hypothesis was supported by the X-Ray analysis of the leaching residues, which did not detect any other Fe precipitates. During the first two periods, there was no precipitation or very little, due to a combination of low pH and low Fe(III) concentration in the liquid phase. During the third period, precipitation was substantial with 0.16 $mmol.h^{-1}$ of sulphates consumed. The amount of Fe(III) precipitating as jarosite was estimated from the consumption of sulphates, given that two moles of sulphates are involved in the formation of jarosite for 3 moles of Fe(III). During the 3rd period, 6.0 $mg.L^{-1}.h^{-1}$ of Fe(III) was consumed by the precipitation phenomena.

- *Generation of Fe(III) by bio-oxidation of Fe(II)*

To estimate the biological Fe(II) bio-oxidation rate, a mass balance for Fe(III) during steady state was calculated for the second stage of the continuous bioreactor:

$$Fe^{3+}_{\text{from bio-oxidation}} = Fe^{3+}_{\text{consumed for leaching}} + Fe^{3+}_{\text{precipitated}} + Fe^{3+}_{\text{in the outlet flow}} - Fe^{3+}_{\text{in the feed}} \qquad [4]$$

Fe(III) concentrations in the feed and the outlet flow ($Fe^{3+}_{\text{in the feed}}$ and $Fe^{3+}_{\text{in the outlet flow}}$) were estimated with the Yue et al. (2016) correlation and AAS results (see Section 2.6). The rate of Fe(III) precipitation ($Fe^{3+}_{\text{precipitated}}$) was estimated from the consumption of sulphates as explained above. The $Fe^{3+}_{\text{consumed for leaching}}$ was estimated from the dissolution rates of the

different metals and the stoichiometric requirements associated with each of these metals (2 moles of Fe(III) for the dissolution of one mole of Cu, 3 moles of Fe(III) per one mole of Al, *etc*.). This calculation was based on the hypothesis that metal were dissolved only by oxidation reactions and acidic hydrolysis was negligible. This hypothesis was supported by the results obtained in the batch bioleaching experiments showing that acidic dissolution is much slower than oxidative dissolution. Concerning Fe dissolution, the Fe contained in PCBs was considered to dissolve as Fe(II) cations, which were potentially re-oxidized; we did not consider Fe dissolution as Fe(III), since the redox potential of the Fe/Fe(III) couple is higher than for Fe/Fe(II). Fe dissolution rate was calculated with the following mass balance on the STR reactor during steady state :

$$Fe_{dissolved} = Fe_{precipitated} + Fe_{in\ the\ leachate} - Fe_{in\ the\ feed} \quad [5]$$

With $Fe_{dissolved}$, $Fe_{in\ the\ feed}$ and $Fe_{in\ the\ leachate}$ the Fe dissolution rate and flows of Fe that came from the bubble column and that went out from STR reactor, respectively. The Fe dissolution rates are shown on Table 8. The estimated Fe dissolution yield reached 93% during the third period. However, the calculated rate of Fe dissolution for the same period of time did not greatly increase. This was due to a small deviation in the solid concentration in the STR, which decreased slowly due to a probable partial obstruction of the dosing screw (less PCBs were added); this deviation was taken into account in our yield calculations.

Consequently, the Fe(III) demand for the dissolution reactions ($Fe^{3+}_{consumed\ for\ leaching}$) varied from 3.63 $mmol.h^{-1}$ (period 1) to 4.96 $mmol.h^{-1}$ (period 3).

Table 8 shows the estimated Fe(II) bio-oxidation rate for each period. These rates increased significantly over the different periods. It should be noted that the balance was calculated on a macroscopic scale. The values will probably vary on a microscopic scale with, for example, areas of high microbial concentration and therefore higher bio-oxidation rates than in our estimations.

	Estimated Fe dissolution yield (%) and rate ($mg.L^{-1}.h^{-1}$)	**Fe(II) bio-oxidation rate ($mg.L^{-1}.h^{-1}$)**
Period 1	76% - 18.7	69
Period 2	62% - 17.2	105
Period 3	93% - 18.5	142

Table 8: Estimation of Fe dissolution kinetics (in % and $mg.L^{-1}.h^{-1}$) and Fe(II) bio-oxidation rates (in $mg.L^{-1}.h^{-1}$) over time in the bioreactor used for continuous bioleaching spent PCBs, in the presence of 1%(w/v) PCBs and HRT=48 h.

➢ *Changes in the bacterial community over time at 1% solids*

To understand the structure of the acidophilic culture and its impact on the different phenomena, various tools were used to characterise the bacterial populations. First, the biomass concentration in the liquid phase was determined with a Thoma cell counting chamber. Figure 10 shows how cell concentrations in the 1st stage and 2nd stage changed over time. During period 1, bacteria were transferred from the bubble column to the second stage of the bioreactor but no growth was observed in the latter. Their concentration in the PCB leaching bioreactor was lower than in the liquid phase at the outlet of the 1st stage. During period 2, the bacteria seemed more active when observed with Thoma cell counting (fast motions on the plate) and slightly more numerous. Finally, during period 3, the number of cells increased sharply in the liquid phase.

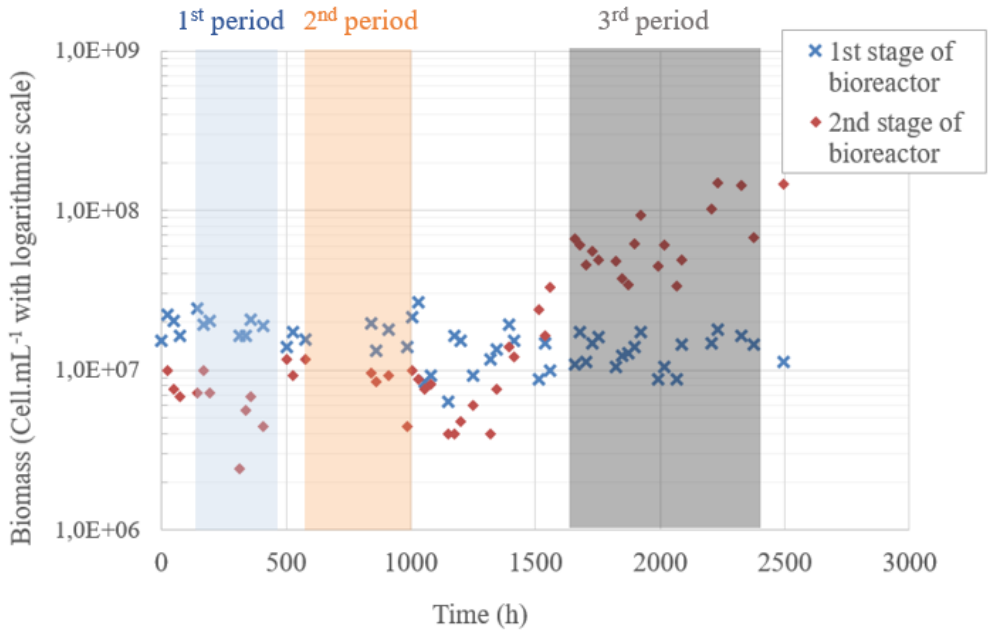

Figure 10: Biomass concentration over time (in cell.mL^{-1}) in the liquid phases of the 1st and 2nd stages of the bioreactor.

DNA extraction in the liquid and solid phases (activated charcoal from the bubble column and comminuted PCB residues in the 2nd stage) enabled us to determine the microbial distribution between the two phases (Figure 11). In the first stage (bubble column), DNA was mainly extracted from activated carbon (99.83%). In the 2nd stage (STR with PCBs), 17% of the DNA was in the liquid phase, while 83% came from the PCBs. Bacteria were mostly attached.

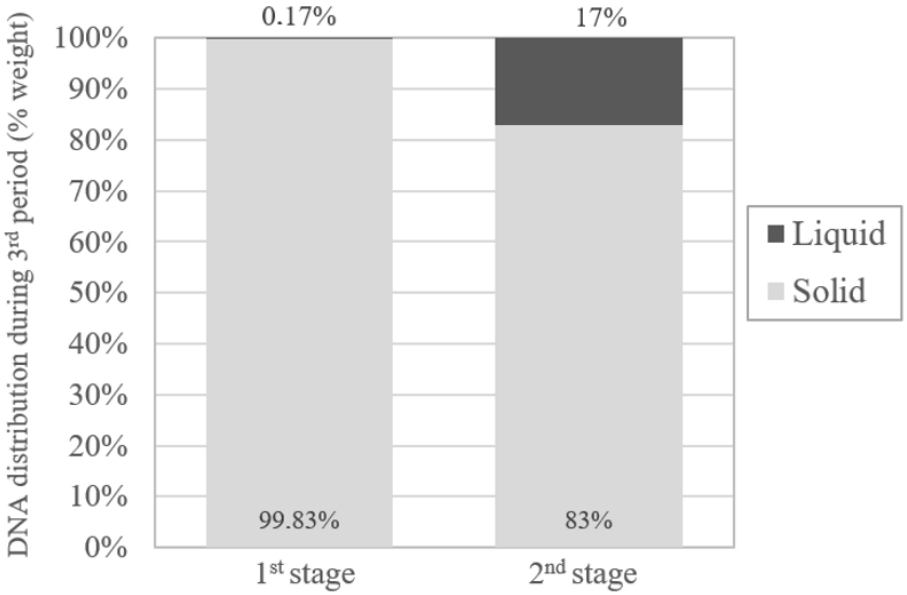

Figure 11: DNA distribution (in % weight) between the liquid and solid phases in the two stages of the continuous bioreactor used for bioleaching spent PCBs.

Microbial diversity profiles in the bioreactors were determined during the 3rd period by 16S rRNA gene CE-SSCP fingerprints. In the first stage (bubble column), the iron-oxidizer *Leptospirillum ferriphilum* was detected at average proportions of 70.4% in the solid phase and 69.3% in the liquid phase. The sulphur and iron oxidizer *Sulfobacillus benefaciens* and an unknown strain were also detected on the solid phase at a relative abundance of 16.5% and 13.1% respectively, and 15.0% and 15.6% respectively on the liquid phase. In the second stage (STR), the growth of *Leptospirillum ferriphilum* was favoured, since only this strain was detected on the fingerprints in the pulp, on the solid phase and in the liquid phase. Despite the fact that *Acidithiobacillus caldus* and *Sulfobacillus thermosulfidooxidans* were known to be members of BRGM-KCC consortium inoculated into the bioreactor, they remained undetected. For *Acidithiobacillus caldus*, which is a sulphur-oxidizing bacterium, this can be explained by the absence of reduced sulphur compounds in the bioreactor. Likewise, the temperature maintained at 35 °C in the bioreactor was probably too low for *Sulfobacillus thermosulfidooxidans* since the optimum growth temperature is 51 °C for this bacterium (Watling et al., 2008).

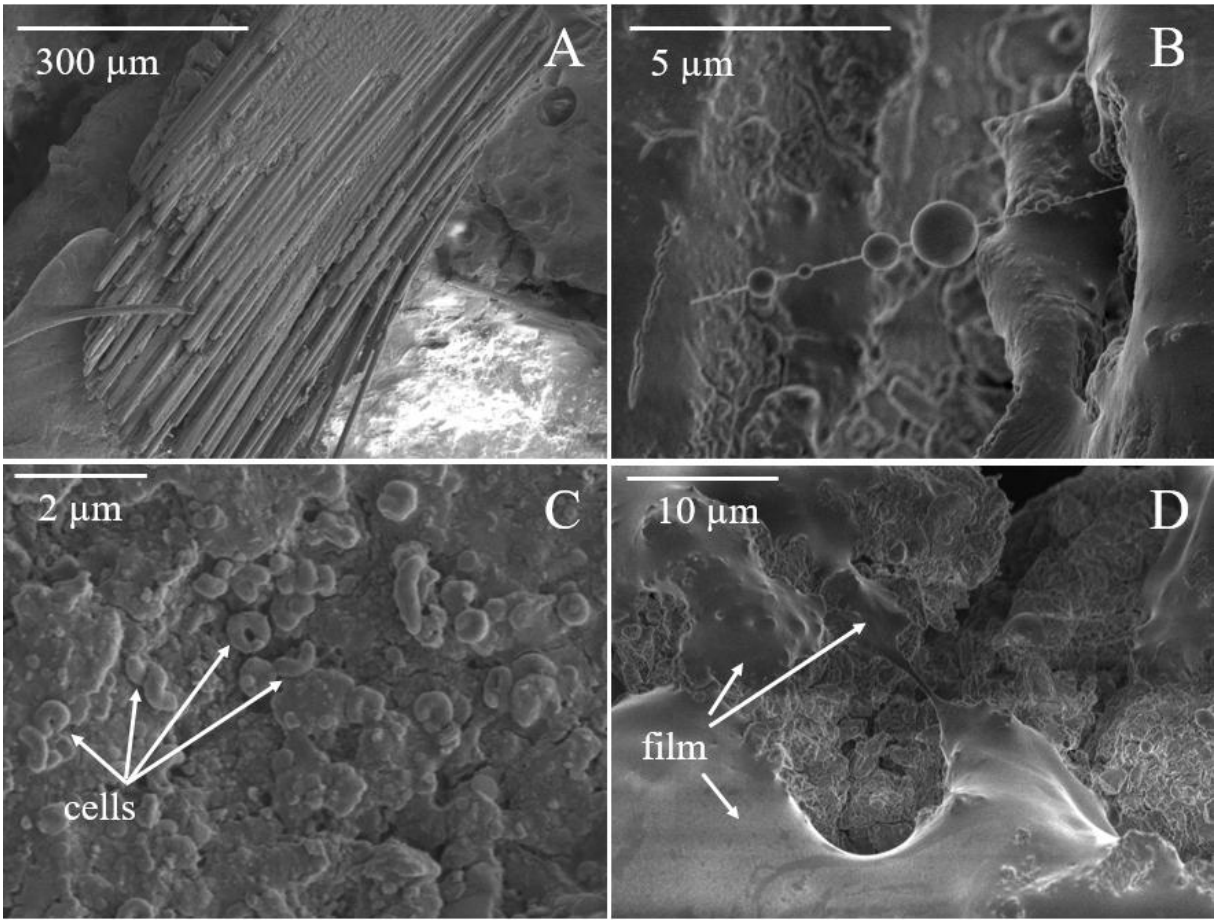

Figure 12: SEM images of different PCB particles that were lyophilised.

Since most of the cells were attached to the PCBs, SEM was used to correlate the presence of attached cells with the composition of the solid phase (Figure 12). Ten PCB fragments were observed. On some fragments, which were probably glass or ceramic fibres made up of Al, Si and Ca (Figure 12A), there was little or no bacteria. Round and organic elements appeared to be attached between some fibres (Figure 12B). A wire linked these elements to the PCB fragment but broke under the electron beam. These elements may be cells that formed spores to protect themselves from their environment: the genus *Sulfobacillus* is able to sporulate for example (Johnson et al., 2008, Watling et al., 2008). On other fragments, containing Br, Si, O, Cu, P, S and Fe (Figure 12C), which were perhaps ceramics covered with jarosite precipitates, there were many cells concentrated in limited areas. These were small and often folded back on themselves. Cells were also detected on plastic fragments (essentially made up of C and O). It was not possible to take pictures of these fragments because they accumulate electrostatic charges from the electron beam despite the metallisation of the sample. Finally, films were detected on some other fragments (Figure 12D), but it was not possible to determine whether they were derived from the microbial activity or from lyophilisation of the

ionic solution. These observations did not enable us to confirm that bacteria became preferentially attached to certain fragments, as asserted by Silva et al. (2015).

- *Bioleaching kinetics at higher concentrations of solids (1.8% w/v)*

When the second stage of the bioreactor reached a permanent regime (stabilisation of all the chemical, physical and biological parameters), the concentration of solids was increased from 1% to 1.8%(w/v). The metal dissolution rates reached with the new concentration are shown in Figure 13: after the change in concentration, they increased gradually and stabilised after 1000 hours. The dissolution rates increased with the concentration of solids for almost all metals (Cu, Fe, Ni, Zn, Sn, Pb, Mn, Co, Al, Cr and Mo) except Ag and Sb. The dissolution rate of Sb remained constant. The dissolution rate of Ag was halved while its concentration in the leachate remained constant. This may be due to precipitation phenomena.

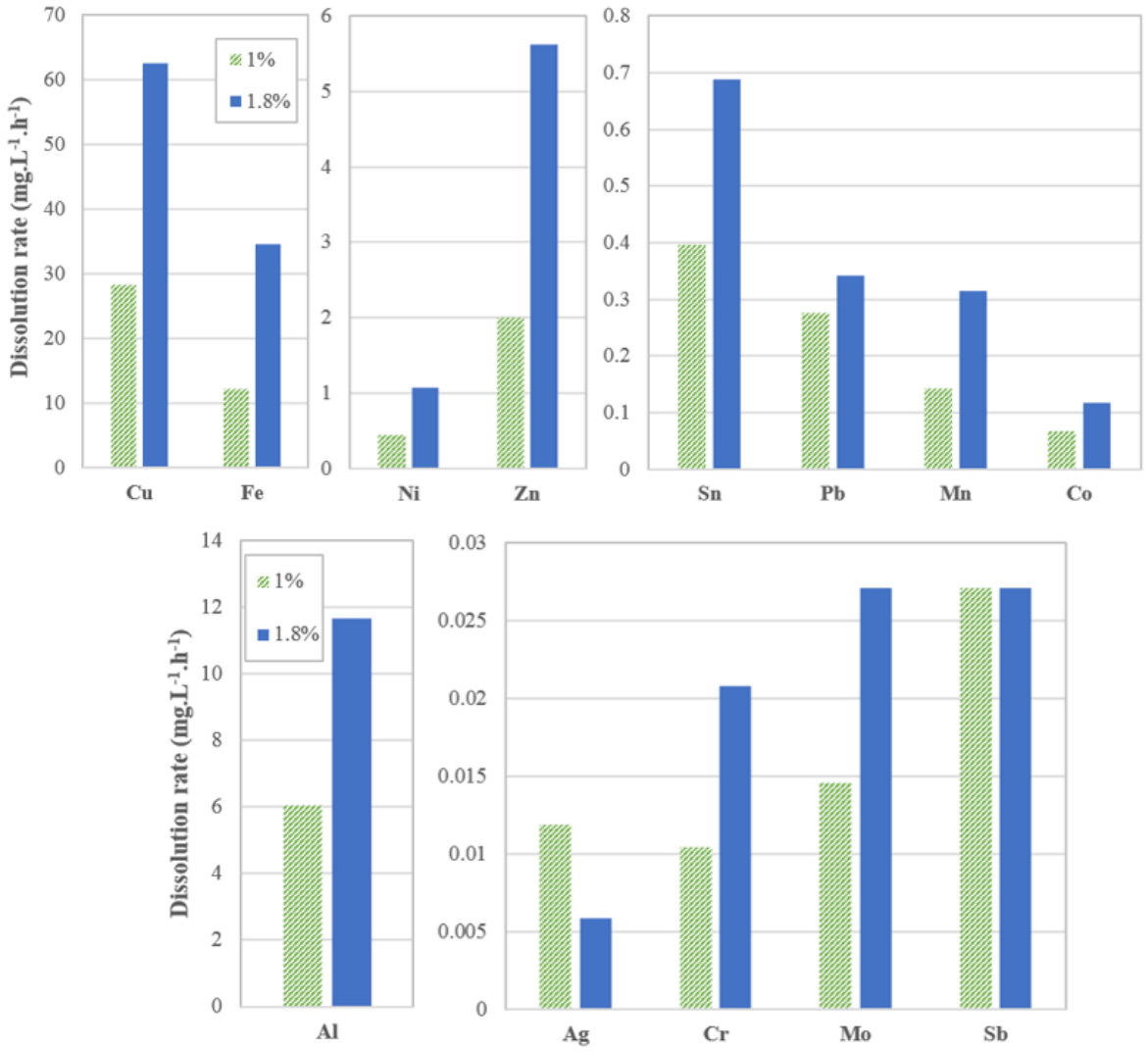

Figure 13: Bioleaching rates (in mg.L^{-1}.h^{-1}) according to the concentration of solids in the double-stage bioreactor run in continuous mode.

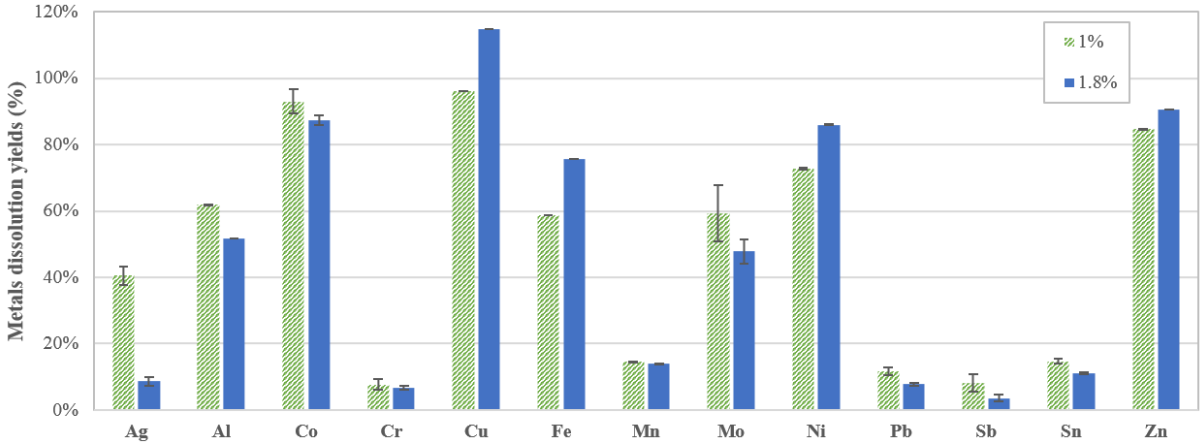

Figure 14: Bioleaching yields (in %) according to the concentration of solids in the double-stage bioreactor run in continuous mode. Error bars depict uncertainties in the leachate analysis.

Figure 14 shows the maximum metal dissolution yields reached after changing the concentration of solids. Some metals such as Ta, W, Ga and V are not reported. In the case of Ta, W and Ga, the analytical uncertainties were still higher than the maximum concentration that would be reached if they were completely dissolved. In the case of V, the limit of detection was 0.1 $mg.L^{-1}$. This value corresponds to a dissolution of 25% of V from PCBs. As V remained undetected, its dissolution yield was thus lower than 25%. The dissolution yields of the other metals were of the same order of magnitude as those reached with the 1%(w/v) concentration of solids, except for Cu whose dissolution yield was above 100% (as explained in batch experiments in Section 3.2, Cu content in PCBs was probably underestimated).

The redox potential was higher than 880 mV vs ENH for both concentrations of solids (data not shown), which shows that all Fe(II) produced by the dissolution of metals in the PCBs was re-oxidized by the microorganisms present in the reactor, the bio-oxidation rate being higher than the rate of Fe(III) consumption.

Using equations [4] and [5], the Fe mass balance was established and the rates of jarosite precipitation and Fe(II) bio-oxidation were estimated (Table 9). For both concentrations of solids, the Fe dissolution yields were very high. They even reached more than 100% at 1.8%(w/v), probably because of an overestimation of jarosite precipitation in our mass balance based on equation [5]: sulphates were apparently involved not only in the precipitation of jarosite but also of anglesite ($PbSO_4$), as shown previously. These high Fe dissolution yields are promising as regards the ability to run the bioreactor without any Fe in the feeding solution, using PCBs as the only source of Fe.

Moreover, the Fe(II) bio-oxidation rate at 1.8%(w/v) was approximately twice the rate obtained at 1%(w/v).

PCB concentration	Fe dissolution rate ($mg.L^{-1}.h^{-1}$)	Fe dissolution yield (%)	Fe(II) bio-oxidation rate ($mg.L^{-1}.h^{-1}$)
1%(w/v)	18.2	93%	142
1.8%(w/v)	61.9	>100%	328

Table 9: Estimation of the Fe(II) bio-oxidation rate (in $mg.L^{-1}.h^{-1}$) and dissolution kinetics of Fe (taking into account jarosite precipitation) according to PCB concentrations.

Figure 15 shows the consumption of protons and the difference in biomass concentrations between the 1st and 2nd stages for different concentrations of solids. The values increased with increasing PCB concentrations. The consumption of protons was due to the high alkalinity of the PCBs and the high bio-oxidation rates. Concerning biomass concentrations, the PCBs did not inhibit bacterial growth. The significant increase in biomass concentrations probably resulted from larger quantities of substrate and from better adaptation of microbial cells to their environment. *Leptospirillum ferriphilum* was the only strain detected in the second stage of the bioreactor (STR) with CE-SSCP fingerprints, as at the 1%(w/v) PCB concentration.

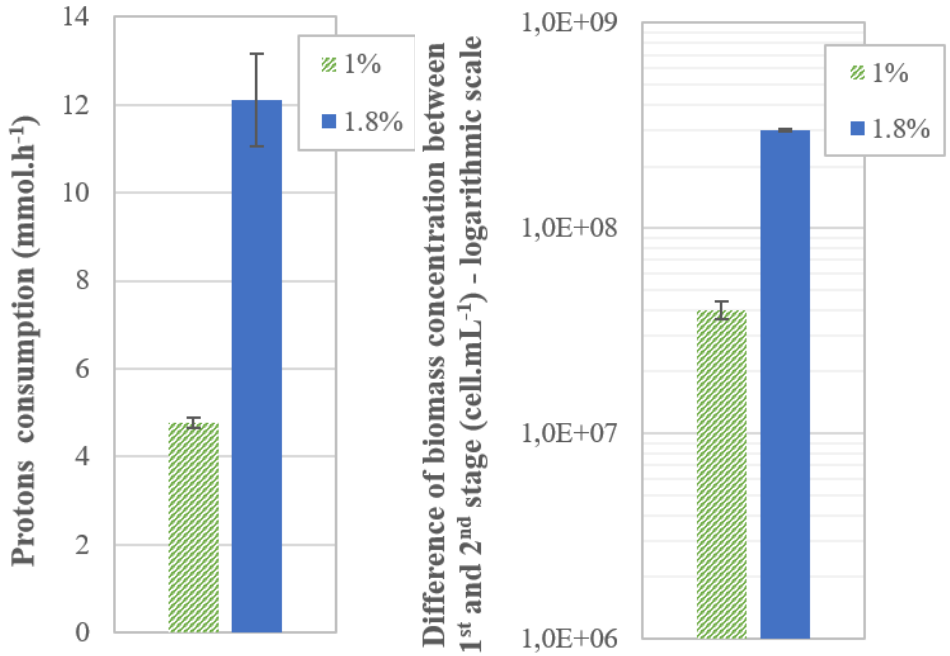

Figure 15: Proton consumption (in mmol.h^{-1}) and difference in bacterial concentrations between the liquid phases of the 1st and 2nd stages (in cell.mL^{-1}, logarithmic scale) for different concentrations of solids.

3.4 Bioleaching of PCBs in continuous mode in a single-stage bioreactor

When the bioreactor reached a stationary state after changing the concentration of solids, the first stage (bubble column) was by-passed and the STR was fed only with the comminuted PCBs and the 0Cm nutritive medium at pH 1.2, without Fe. The aim was to test the ability of the bacteria in the bioreactor to use PCBs as the only source of Fe, since the Fe content in the PCBs had reached 12.2% (in weight). The concentration of solids was maintained at 1.8% (w/v). The dissolution yields reached in the single-stage bioreactor were compared to those obtained during the double-stage experiment and are given in Figure 16. Proton consumption and biomass concentration in the liquid phase are shown in Figure 17. Redox potential is not shown but remained the same after the first stage was by-passed. These results clearly indicate that there was no major difference between the two modes of operation. A slight improvement was even observed in the dissolution yields of Cu, Fe, Zn, Ni and Co. Slightly higher consumption of protons was observed when the 1st stage was no longer being operated. It also seemed that the culture was less robust to possible changes in operating conditions, such as air shutdowns: when a sudden change in operating conditions occurred, the time needed to obtain similar dissolution yields after favourable conditions were restored was longer than when the first stage was not by-passed (data not shown).

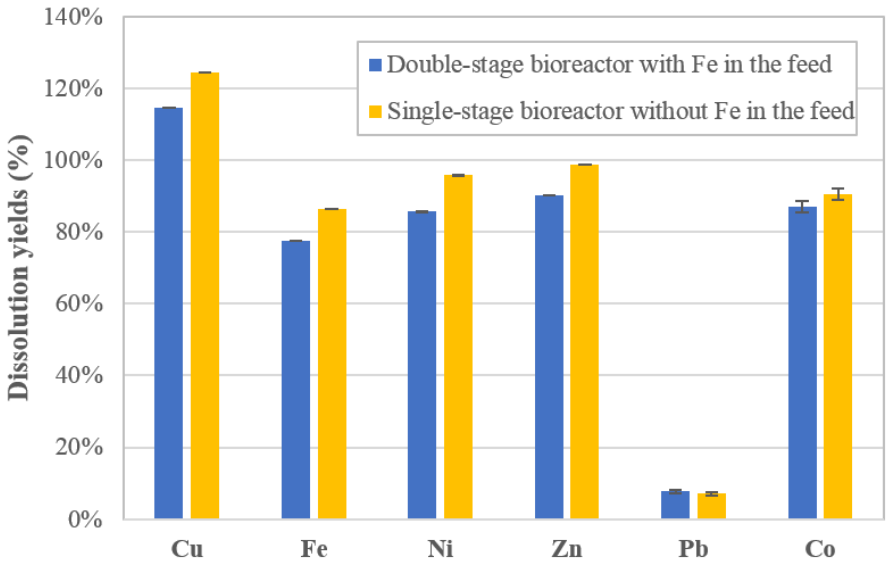

Figure 16: Cu, Fe, Zn, Ni, Pb and Co dissolution yields (in %) in the presence of 1.8%(w/v) PCBs in the double-stage bioreactor with 1 g.L^{-1} Fe(II) in the feed and in the single-stage bioreactor (by-pass of the bubble column) without Fe in the feed.

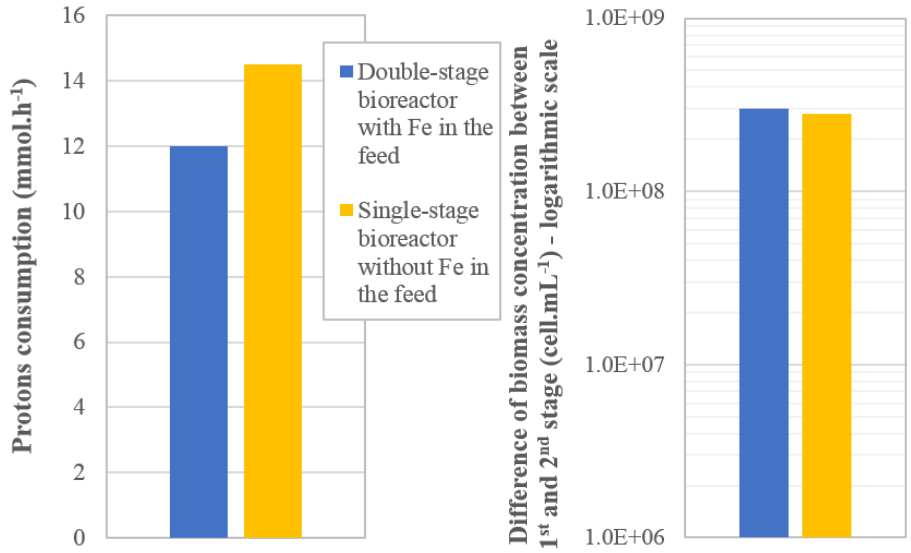

Figure 17: Proton consumption (in mmol.h^{-1}) and difference in biomass concentrations between the 1st and 2nd stage (in cell.mL^{-1}, logarithmic scale) in the presence of 1.8%(w/v) PCBs in the double-stage bioreactor with 1 g.L^{-1} Fe(II) in the feed and in the single-stage bioreactor (by-pass of the bubble column) without Fe in the feed.

4. Discussion

➢ *Toxicity test and bioleaching in batch mode*

Although the bioleaching kinetics in batch mode were quite conclusive, the contribution of the biological compartment to the leaching reactions was not fully demonstrated: the biological activity in the dissolution of metals was almost undetectable during these experiments in batch mode. High initial concentrations of Fe(III) (either biogenic or synthetic) were therefore necessary to obtain rapid kinetics: 7 g.L^{-1} of Fe(III) were necessary in the presence of 1%(w/v) PCBs and 35 g.L^{-1} of Fe(III) would be necessary in the presence of 5%(w/v) of solids. These high Fe concentrations would be difficult to manage in downstream hydrometallurgical operations. Fe(II) bio-oxidation was nevertheless detected after a long lag phase (approximately 300 h), which was also the case during the microbial ecotoxicology tests. The culture would need to be adapted to the e-waste, but this can hardly be done on an industrial scale because of the highly variable composition of e-waste. The transition to the operation in continuous mode eliminated the time-lag as a steady-state mode was established. This allowed metal dissolution and Fe(II) bio-oxidation to be observed simultaneously.

➢ *PCB bioleaching in continuous mode*

At the beginning of the study on PCB bioleaching in continuous mode with 1%(w/v) PCBs, three distinct periods were observed, which could be attributed to phases in cell adaptation:

- **Period 1 (0 – 400 h)**: Bacteria entering the second stage (STR) were not able to grow or to oxidize Fe(II) noticeably. Metal dissolution was mainly related to chemical leaching by incoming Fe(III) (1 $g.L^{-1}$) and sulphuric acid. Thus, consumption of 1.7 $mmol.h^{-1}$ of protons was observed in the second stage. Our estimation of the Fe(II) bio-oxidation rate (Table 8) gave 69 $mg.L^{-1}.h^{-1}$. It could be assumed that there is a bias on this value due the fact that during this period, leaching was partly caused by hydrolysis reactions with sulphuric acid. This phenomenon, which was not considered in our mass balance, artificially increased Fe(III) demand due to the dissolution of metals and distorted both the mass balance and the evaluation of the bio-oxidation rate.
- **Period 2 (600 – 1000 h)**: The bacteria were slightly more active (cells were more mobile on the counting chamber). Metal dissolution rates and yields increased during this period compared to the previous ones, probably because of the bio-oxidation of Fe(II). However, only Fe(II) was detected: it is likely that the kinetics of Fe(III) generation (bio-oxidation of Fe(II)) were slower than the consumption kinetics. The consumption of protons also increased, which was consistent with the bio-oxidation reaction [2]. In addition, very low consumption of sulphates was observed, which corresponded to a very low rate of jarosite precipitation.
- **Period 3 (1600 – 2400 h)** : The number of cells increased exponentially in the liquid phase. The microbial culture bio-oxidized Fe(II) much faster than the consumption of Fe(III) by the metal dissolution reactions, so that only Fe(III) was detected. Moreover, the addition of sulphuric acid to maintain a low pH (<1.8), SO_4^{2-} and the higher Fe(III) concentrations than during the previous periods favoured the precipitation phenomena and jarosite formation.

Thus, the adaptation time of bacteria was relatively long, but the culture eventually developed in the second stage within a reasonable time. The time to reach period 2 (600 h), when bacterial activity began, was longer than that observed in the shake flasks for the toxicity tests and in batch mode (approximately 300 h). It should be noted, however, that management problems with the experimental reactor in continuous mode (such as air shutdowns) may have

slowed down the adaptation process. Moreover, toxicity tests were performed with PCBs leachates only, while solid particles could extend the adaptation time.

When increasing the concentration of solids to 1.8%(w/v), a gradual increase in dissolution rates was observed. This was probably linked to the gradual adaptation of the bacteria to the new concentration of solids. After 1000 hours, the bacteria had adapted well, so that dissolution yields reached values equivalent to those at 1%(w/v) for most metals and dissolution rates increased overall.

As a result of the tests in the presence of 1.8%(w/v) PCBs in continuous mode in the double-stage bioreactor, it seemed that biomass concentration in the 2nd stage (STR) was sufficient to eliminate the 1st stage and thus simplify the process. The same dissolution kinetics were observed in the double-stage bioreactor supplied with 1 g.L^{-1} Fe(II) and in the single-stage bioreactor supplied with the nutrient solution. The yields obtained were even slightly higher, probably due to better adaptation of bacteria to their environment. Thus, once the bioleaching reaction was established in the bioreactor, the first stage was no longer necessary. Bacteria were able to grow in the second stage. The intake of Fe contained in the PCBs was sufficient, so that no Fe(II) needed to be added to the feeding solution. Consequently, the Fe concentration in the leachates was lower. This is of significant benefit to simplify downstream hydrometallurgical processes, since large quantities of Fe(III) in leachates raise many issues.

The structure of the bacterial population showed that the operating conditions were unsuitable for the growth of *Acidithiobacillus caldus* and *Sulfobacillus thermosulfidooxidans*, as explained in Hubau et al. (2018), although they are known members of the BRGM-KCC consortium inoculated into the bioreactor, while *Sulfobacillus benefaciens* was detected only in the first stage (bubble column) and may sporulate. The iron-oxidizer *Leptospirillum ferriphilum* appeared to be the species most suited to PCB bioleaching conditions in the STR. A high rate of cell attachment to PCB fragments was also apparent. This may be related to their usual disposition: for example, *Leptospirillum ferriphilum* is most often present in larger proportions on solid fractions than in plankton form (Guezennec et al., 2017). It was also consistent with the study by Silva et al. (2015), which indicated a high rate of cell attachment during bioleaching of PCBs.

Finally, it appeared that the rates of metal dissolution obtained in continuous mode at 1%(w/v) (Table 7) were much lower than the maximum rates obtained in batch mode (Table 4) in the presence of excess Fe(III) (factor 21 for Cu and Ni, 45 for Fe, 57 for Zn, 36 for Fe, Pb and 40 for Co). This was also confirmed at 1.8% (w/v). It can therefore be assumed that

operating conditions in continuous mode could be modified to increase the dissolution rates further: either the hydraulic residence time could be decreased, or the PCB concentration could be increased. This is also consistent with the fact that the estimated Fe(II) bio-oxidation rates in continuous mode were very low (142 $mg.L^{-1}.h^{-1}$ at 1%(w/v) and 328 $mg.L^{-1}.h^{-1}$ at 1.8%(w/v)) compared to the bio-oxidation rate obtained in the bubble column (1400 $mg.L^{-1}.h^{-1}$, Hubau et al., 2018). It seems that limits of dissolution kinetics were not reached in our experiments, which is a promising result for further work.

PCBs contain metals in concentrations much higher than those of conventional ores. This innovative work has demonstrated that the bioleaching of this resource in continuous mode was efficient to recover metals.

5. Conclusion

Acidophilic bioleaching of PCBs in a stirred tank reactor in batch mode gave promising results in the presence of 1% or 5%(w/v) PCBs. The study was conducted in two stages: bacterial growth in the presence of Fe(II) oxidized into Fe(III), followed by the addition of PCBs. Metals were quickly dissolved in the presence of an excess of Fe(III). However, the study could not show the impact of microbial Fe(III) regeneration on metal dissolution kinetics because their lag phase was longer than the time typically required for their chemical dissolution. Moreover, in batch mode, the bacteria were able to oxidize Fe(II) in the presence of 1%(w/v) PCBs but not 5%(w/v).

Setting up a continuous double-stage bioreactor enabled us to adapt the culture to PCBs so that Fe(III) was regenerated: at start-up, the culture could not become active in the PCB reactor, but after a few weeks, biomass concentrations greatly exceeded concentrations in the incoming flow and all the Fe was in the form of Fe(III). Consequently, although Fe(III) was not in excess in the feeding solution, the main metals were dissolved in 48 hours with high yields: 96% Cu, 85% Zn, 73% Ni, 93% Co and an estimated 93% of Fe (taking into account its precipitation as jarosite). The Pb dissolution yield only reached 12% because it precipitated as anglesite ($PbSO_4$). Bacteria were mainly attached to solid particles, perhaps to better withstand the stress of their environment containing high concentrations of metal cations. Their attachment did not seem to be specific to the composition of the particle (plastics, ceramics, etc.). *Leptospirillum ferriphilum* seemed to be better adapted and more resistant than other species in such conditions.

Increasing the concentration of solids to 1.8%(w/v) resulted in higher dissolution rates. The culture adapted rapidly to the higher concentration of PCBs and the biomass concentration was even greater. After several months of operation, this made it possible to withdraw the 1st stage without affecting the bioleaching kinetics. Moreover, the experiments showed that it was no longer necessary to provide Fe(II) in the feeding solution, as the bacteria were able to use Fe from PCBs only, even though the culture seemed to be more sensitive to sudden variations in operating conditions. These points were beneficial for the economy of the process. This study opens up new perspectives about continuous bioleaching of PCBs. It would be necessary to study the impacts on dissolution kinetics of solids at higher concentrations or at shorter residence times.

6. Acknowledgements

This study was supported by the “Mines Urbaines” Chair of the ParisTech foundation supported by Eco-systèmes.

7. References

Adhapure, N.N., Waghmare, S.S., Hamde, V.S., Deshmukh, A.M., 2013. Metal Solubilization from Powdered Printed Circuit Boards by Microbial Consortium from Bauxite and Pyrite Ores, Applied Biochemistry and Microbiology, 49, 3, 256–262.

AFNOR, 2014. Water quality - Determination of selected parameters by discrete analysis systems - Part 1: Ammonium, nitrate, nitrite, chloride, orthophosphate, sulfate and silicate with photometric detection, international standard ISO 15923-1:2014, 25 p.

Arshadi, M., Mousavi, S.M., 2014. Simultaneous recovery of Ni and Cu from computer printed circuit boards using bioleaching: Statistical evaluation and optimization, Bioresource Technology, 174, 233–242.

Arshadi, M., Mousavi, S.M., 2015. Multi-objective optimization of heavy metals bioleaching from discarded mobile phone PCBs: Simultaneous Cu and Ni recovery using Acidithiobacillus ferrooxidans, Separation and Purification Technology, 147, 210–219.

Bai, J., Wang, J., Xu, J., Zhou, M., Guan, J., Zhang, C., 2009. Microbiological recovering of metals from printed circuit boards by Acidithiobacillus ferrooxidans, Proceedings for the IEEE International Symposium on Sustainable Systems and Technology.

Bai, J., Gu, W., Dai, J., Zhang, C., Yuan, W., Deng, M., Luo, X., Wang, J., 2016. The catalytic role of nitrogen-doped carbon nanotubes in bioleaching copper from waste printed circuit boards, Pol. J. Environ. Stud., 25 (3), 951-957.

Bas, A.D., Deveci, H., Yazici, E.Y., 2013. Bioleaching of copper from low grade scrap TV circuit boards using mesophilic bacteria, Hydrometallurgy, 138, 65–70.

Brandl, H., Bosshard, R., Wegmann, M., 2001. Computer-munching microbes: metal leaching from electronic scrap by bacteria and fungi. Hydrometallurgy 59, 319–326.

Bryan, C.G., Watkin, E.L., McCredden, T.J., Wong, Z.R., Harrison, S.T.L., Kaksonen, A.H., 2015. The use of pyrite as a source of lixiviant in the bioleaching of electronic waste, Hydrometallurgy, 152, 33-43.

Cerruti, C., Curutchet, G., Donati, E., 1998. Bio-dissolution of spent nickel–cadmium batteries using Thiobacillus ferrooxidans, Journal of Biotechnology, 62, 209-219.

Chen, S., Yang, Y., Liu, C., Dong, F., Liu, B., 2015. Column bioleaching copper and its kinetics of waste printed circuit boards (WPCBs) by Acidithiobacillus ferrooxidans, Chemosphere, 141, 162-168.

Choi, M.S., Cho, K.S., Kim, D.S., Kim, D.J., 2004. Microbial recovery of copper from printed circuit boards of waste computer by *Acidithiobacillus ferrooxidans*, Journal of environmental science and health, 39:11-12, 2973-2982.

Coram, N.J., Rawlings, D.E., 2002. Molecular relationship between two groups of the genus Leptospirillum and the finding that Leptospirillum ferriphilum sp. nov. dominates South African commercial biooxidation tanks that operate at 40°C, Applied and environmental microbiology, 838-845.

Gu, W., Bai, J., Dai, J., Zhang, C., Yuan, W., Wang, J., Wang, P., Zhao, X., 2014. Characterization of extreme acidophile bacteria (Acidithiobacillus ferrooxidans) bioleaching copper from flexible PCB by ICP-AES, Journal of Spectroscopy, 269351.

Gu, W., Bai, J., Dong, B., Zhuang, X., Zhao, J., Zhang, C., Wang, J., Shih, K., 2017a. Catalytic effect of graphene in bioleaching copper from waste printed circuit boards by Acidithiobacillus ferrooxidans, Hydrometallurgy, 171, 172-178.

Gu, W., Bai, J., Dong, B., Zhuang, X., Zhao, J., Zhang, C., Wang, J., Shih, K., 2017b. Enhanced bioleaching efficiency of copper from waste printed circuit board driven by

nitrogen-doped carbon nanotubes modified electrode, Chemical Engineering Journal, 324, 122-129.

Guezennec, A.G., Bru, K., Jacob, J., d'Hugues, P., 2015. Co-processing of sulfidic mining wastes and metal-rich post-consumer wastes by biohydrometallurgy, Minerals Engineering, 75, 45–53.

Guezennec, A.G., Joulian, C., Delort, C., Bodénan, F., Hedrich, S., d'Hugues, P., 2018. CO_2 mass transfer in bioleaching reactors: CO_2 enrichment applied to a complex copper concentrate, Hydrometallurgy, 180, 277-286.

Guezennec, A.G., Joulian, C., Jacob, J., Archane, A., Ibarra, D., de Buyer, R., Bodénan, F., d'Hugues, P., 2017. Influence of dissolved oxygen on the bioleaching efficiency under oxygen enriched atmosphere, Minerals Engineering, 106, 64–70.

Gy, P.M. 1992. Sampling of heterogeneous and dynamic material systems, theories of heterogeneity, sampling and homogeneizing, Elsevier, Amsterdam, 653p.

Hedrich, S., Guezennec, A.-G., Charron, M., Schippers, A., Joulian, C., 2016. Quantitative Monitoring of Microbial Species during Bioleaching of a Copper Concentrate, Frontiers in Microbiology, 07, 2044.

Hubau, A., Chagnes, A., Minier, M., Touzé, S., Chapron, S., Guezennec, A.G., 2019. Recycling-oriented methodology to sample and characterize the metal composition of waste Printed Circuit Boards, Waste Management, 91, 62-71.

Hubau, A., Minier, M., Chagnes, A., Joulian, C., Perez, C., Guezennec, A.G., 2018. Continuous production of a biogenic ferric iron lixiviant for the bioleaching of printed circuit boards (PCBs), Hydrometallurgy, 180, 180-191.

Ilyas, S., Anwar, M.A., Niazi, S.B., Ghauri, M.A., 2007. Bioleaching of metals from electronic scrap by moderately thermophilic acidophilic bacteria, Hydrometallurgy, 88, 180–188.

Ilyas, S., Lee, J.C., 2014. Bioleaching of metals from electronic scrap in a stirred tank reactor, Hydrometallurgy, 149, 50–62.

Ilyas, S., Lee, J.C., Chi, R.A., 2013. Bioleaching of metals from electronic scrap and its potential for commercial exploitation, Hydrometallurgy, 131-132, 138–143.

Ilyas, S., Ruan, C., Bhatti, H. N., Ghauri, M. A., Anwar, M. A., 2010. Column bioleaching of metals from electronic scrap, Hydrometallurgy 101, 135–140.

Işildar, A., van de Vossenberg, J., Rene, E.R., van Hullebusch, E.D., Lens, P.N.I., 2015. Two-step bioleaching of copper and gold from discarded printed circuit boards (PCB), Waste Management, 57, 149-157.

Johnson, D. B., Joulian, C., d'Hugues, P., Hallberg, K. B., 2008. Sulfobacillus benefaciens sp. nov., an acidophilic facultative anaerobic Firmicute isolated from mineral bioleaching operations, Extremophiles, 12, 789–798.

Liang, G., Mo, Y., Zhou, Q., 2010. Novel strategies of bioleaching metals from printed circuit boards (PCBs) in mixed cultivation of two acidophiles, Enzyme and Microbial Technology, 47, 322–326.

Liang, G., Tang, J., Liu, W., Zhou, Q., 2013. Optimizing mixed culture of two acidophiles to improve copper recovery from printed circuit boards (PCBs), Journal of Hazardous Materials, 250-251, 238–245.

Liang, G., Ti, P., Liu, W., Wang, B., 2016. Enhanced bioleaching efficiency of copper from waste printed circuit boards (PCBs) by dissolved oxygen-shifted strategy in Acidithiobacillus ferrooxidans, J Mater Cycles Waste Manag, 18, 742-751.

Mäkinen, J., Bachér, J., Kaartinen, T., Wahlström, M., Salminen, J., 2015. The effect of flotation and parameters for bioleaching of printed circuit boards, Minerals Engineering, 75, 26–31.

Mrážiková, A., Marcinčáková, R., Kaduková, J., Velgosová, O., 2013. Influence of bacterial culture to copper bioleaching from printed circuit boards, J. Polish Mineral Engineering Scoiety, 59-62.

Mrážiková, A., Marcinčáková, R., Kaduková, J., Velgosová, O., Balintova, M., 2015. Influence of used bacterial culture on zinc and aluminium bioleaching from printed circuit boards, Nova Biotechnologica et Chimica, 14-1, 45-51.

Mrážiková, A., Kaduková, J., Marcinčáková, R., Velgosová, O., Willner, J., Fornalczyk, A., Saternus, M., 2016. The effect of specific conditions on Cu, Ni, Zn and Al recovery from PCBs waste using acidophilic bacterial strains, Arch. Metall. Mater., 61, 1, 261–264.

Nie, H., Yang, C., Zhu, N., Wu, P., Zhang, T., Zhang, Y., Xing, Y., 2014. Isolation of Acidithiobacillus ferrooxidans strain Z1 and its mechanism of bioleaching copper from waste printed circuit boards, J. Chem. Technol. Biotechnol., 90, 714-721.

Nie, H., Zhu, N., Cao, Y., Xu, Z., Wu, P., 2015. Immobilization of Acidithiobacillus ferrooxidans on Cotton Gauze for the Bioleaching ofWaste Printed Circuit Boards, Appl Biochem Biotechnol, 177, 675–688.

Priya, A., Hait, S., 2018. Extraction of metals from high grade waste printed circuit board by conventional and hybrid bioleaching using Acidithiobacillus ferrooxidans, Hydrometallurgy, 177, 132-139.

Rodrigues, M.L.M., Leão, V.A., Gomes, O., Lambert, F., Bastin, D., Gaydardzhiev, S., 2015. Copper extraction from coarsely ground printed circuit boards using moderate thermophilic bacteria in a rotating-drum reactor, Waste Management, 41, 148-158.

Shah, M.B., Tipre, D.R., Dave, S.R., 2014. Chemical and biological processes for multi-metal extraction from waste printed circuit boards of computers and mobile phones, Waste Management & Research, 32(11), 1134-1141.

Shah, M.B., Tipre, D.R., Purohit, M.S., Dave, S.R., 2015. Development of two-step process for enhanced biorecovery of Cu-Zn-Ni from computer printed circuit boards, Journal of Bioscience and Bioengineering, 120(2), 167-173.

Silva, R.A., Park, J., Lee, E., Park, J., Choi, S.Q., Kim, H., 2015. Influence of bacterial adhesion on copper extraction from printed circuit boards, Separation and Purification Technology, 143, 169–176.

Sodha, A.B., Qureshi, S.A., Khatri, B.R., Tipre, D.R., Dave, S.R., 2017. Enhancement in Iron Oxidation and Multi-metal Extraction from Waste Television Printed Circuit Boards by Iron Oxidizing Leptospirillum ferriphilum Isolated from Coal Sample, Waste Biomass Valor, 1-10.

Sum, E.Y.L., 1991. The recovery of metals from electronic scrap, Review of Extractive Metallurgy, JOM, 53-61.

Tuncuk, A., Stazi, V., Akcil, A., Yazici, E. Y., Deveci, H., 2012. Aqueous metal recovery techniques from e-scrap: Hydrometallurgy in recycling, Miner. Eng., 25, 28–37.

Wang, J., Bai, J., Liang, B., 2009. Bioleaching of metals from printed wire boards by Acidithiobacillus ferrooxidans and Acidithiobacillus thiooxidans and their mixture, Journal of Hazardous Materials, 172, 1100-1105.

Wang, L., Li, Q., Li, Y., Sun, X., Li, J., Shen, J., Han, W., Wang, L. 2018. A novel approach for recovery of metals from waste printed circuit boards and simultaneous removal of iron from steel pickling waste liquor by two-step hydrometallurgical method, Waste Management, 71, 411-419.

Wang, S., Zheng, Y., Yan, W., Chen, L., Mahadevan, G.D., Zhao, F., 2016. Enhanced bioleaching efficiency of metals from E-wastes driven by biochar, Journal of Hazardous Materials, 320, 393-400.

Watling, H. R., Perrot, F. A., Shiers, D. W., 2008. Comparison of selected characteristics of Sulfobacillus species and review of their occurrence in acidic and bioleaching environments. Hydrometallurgy, 93, 57–65.

Willner, J., 2013. Influence of physical and chemical factors on biological leaching process of copper from printed circuit boards, Metabk, 52(2), 189-192.

Willscher, S., Katzschner, M., Jentzsch, K., Matys, S., Pöllmann, H., 2007. Microbial leaching of metals from printed circuit boards, Advanced Materials Research, 20-21, 99-102.

Xia, M.C., Wang, Y.P., Peng, T.J., Shen, L., Yu, R.L., Liu, Y.D., Chen, M., Li, J.K., Wu, X.L., Zeng, W.M., 2017. Recycling of metals from pretreated waste printed circuit boards effectively in stirred tank reactor by a moderately thermophilic culture, Journal of Bioscience and Bioengineering, 123(6), 714-721.

Xiang, Y., Wu, P., Zhu, N., Zhang, T., Liu, W., Wu, J., Li, P., 2010. Bioleaching of copper from waste printed circuit boards by bacterial consortium enriched from acid mine drainage, Journal of Hazardous Materials, 184, 812–818.

Yamane, L.H., Moraes, V.T., Tenório, J.A.S., Espinosa, D.C.R., 2018. Influence of Bacterial Adaptation on Copper Bioleaching from Printed Circuit Boards, Adv Biotech & Micro, 9(3), 555761.

Yang, T., Xu, Z., Wen, J., Yang, L., 2009. Factors influencing bioleaching copper from waste printed circuit boards by Acidithiobacillus ferrooxidans, Hydrometallurgy, 97, 29-32.

Yang, Y., Chen, S., Li, S., Chen, M., Chen, H., Liu, B., 2014. Bioleaching waste printed circuit boards by Acidithiobacillus ferrooxidans and its kinetics aspect, Journal of Biotechnology, 173, 24–30.

Yue, G., Guezennec, A.G., Asselin, E., 2016. Extended validation of an expression to predict ORP and iron chemistry: Application to complex solutions generated during the acidic leaching or bioleaching of printed circuit boards, Hydrometallurgy, 164, 334-342.

Zhu, N., Xiang, Y., Zhang, T., Wu, P., Dang, Z., Li, P., Wu, J., 2011. Bioleaching of metal concentrates of waste printed circuit boards by mixed culture of acidophilic bacteria, Journal of Hazardous Materials, 192, 2, 614-619.